

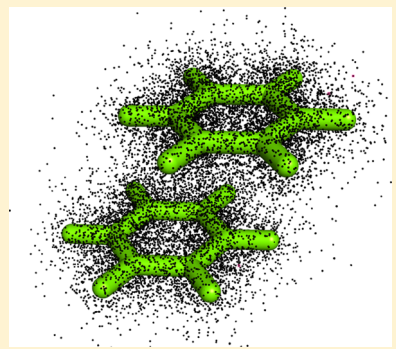
Noncovalent Interactions by Quantum Monte Carlo

Matúš Dubecký,*[†] Lubos Mitas,*[‡] and Petr Jurečka[†]

[†]Regional Centre of Advanced Technologies and Materials, Department of Physical Chemistry, Faculty of Science, Palacký University Olomouc, tř. 17 listopadu 12, 771 46 Olomouc, Czech Republic

[‡]Department of Physics and CHIPS, North Carolina State University, Raleigh, North Carolina 27695, United States

ABSTRACT: Quantum Monte Carlo (QMC) is a family of stochastic methods for solving quantum many-body problems such as the stationary Schrödinger equation. The review introduces basic notions of electronic structure QMC based on random walks in real space as well as its advances and adaptations to systems with noncovalent interactions. Specific issues such as fixed-node error cancellation, construction of trial wave functions, and efficiency considerations that allow for benchmark quality QMC energy differences are described in detail. Comprehensive overview of articles covers QMC applications to systems with noncovalent interactions over the last three decades. The current status of QMC with regard to efficiency, applicability, and usability by nonexperts together with further considerations about QMC developments, limitations, and unsolved challenges are discussed as well.



CONTENTS

1. Introduction	5188	4.10. Open-Shell and Multireference Complexes	5207
1.1. Benchmark Calculations	5189	4.11. Fundamental Insight and Theory	5208
1.2. Why Quantum Monte Carlo?	5190	5. Discussion and Challenges	5208
1.3. Review Scope	5191	6. Conclusions	5208
2. Quantum Monte Carlo (QMC)	5191	Author Information	5209
2.1. Diffusion Monte Carlo for Electrons	5191	Corresponding Authors	5209
2.2. Trial Wave Functions	5193	Notes	5209
2.3. Optimization of Trial Wave Functions	5194	Biographies	5209
2.4. Effective Core Potentials	5194	Acknowledgments	5209
2.5. Treatment of Periodicity	5195	References	5209
2.6. Scaling and Related QMC Methods	5196		
2.7. Practical QMC Computations	5196		
3. Noncovalent Interactions by QMC	5197	1. INTRODUCTION	
3.1. Specific Considerations	5197	Noncovalent interactions are abundant in nature ^{1,2} and are very important in many research areas such as chemistry, ^{2–6} biology, ⁷ biochemistry, ^{2,8} molecular recognition, ⁹ drug design, ^{10–12} materials science, ^{13–15} and beyond. Due to their technological and fundamental importance, noncovalent interactions are studied very extensively using a broad range of experimental, theoretical, and computational approaches. ^{13,16,17} In particular, theory and computations are indispensable not only for understanding, interpretation, and validation of experimental measurements but also for obtaining information that is complementary to what is accessible in experiments. ¹⁸ Noncovalent interaction studies therefore often combine experiments with theory ^{19,20} in order to gain more comprehensive insights and deeper fundamental understanding.	
3.2. Fixed-Node Bias Cancellation	5197	There are many distinct types of noncovalent interactions that differ in their origin or nature of the interacting species. Hydrogen bonding and stacking (or $\pi-\pi$ interaction) are	
3.3. Practical Aspects	5200		
3.3.1. Trial Wave Functions	5200		
3.3.2. One-Particle Orbitals	5200		
3.3.3. Basis Sets	5201		
3.3.4. Explicit Correlation	5202		
3.3.5. Variational Cost Function	5202		
3.3.6. Diffusion Monte Carlo	5202		
3.3.7. Summary	5203		
4. Applications	5203		
4.1. Hydrogen and Hydrogen Storage	5204		
4.2. Noble Gases	5204		
4.3. Water and Ice	5204		
4.4. Carbon-Based Systems	5205		
4.5. Biomolecular Complexes	5206		
4.6. Host–Guest Complexes	5206		
4.7. Small Molecular Complexes	5206		
4.8. Nanomaterials	5207		
4.9. Crystals and Surfaces	5207		

Special Issue: Noncovalent Interactions

Received: September 30, 2015

Published: April 15, 2016

perhaps the most studied as they play important roles in the structural biology of nucleic acids and proteins. In addition, many more interaction patterns were identified over the years, such as halogen bond, sigma hole interaction, blue-shifting hydrogen bond, dihydrogen bond, or anion/cation- π interaction to name just a few. For a more complete classification of noncovalent interactions see, for example, ref 18. From the theoretical viewpoint, noncovalent interactions are best understood in terms of electrostatic, induction (or polarization), dispersion, and exchange-repulsion components, whose balance determines the total intermolecular interaction potential.²¹ Electrostatic interactions originate from the classical Coulomb interaction of the monomer electron distributions (unperturbed by the interaction). Induction is the change in the electrostatic interaction due to polarization of the monomer charge density by the interacting molecules. Dispersion arises from the interaction of the instantaneous fluctuations of the electronic density and the multipoles induced by this fluctuation. At short distance, the attractive forces are opposed by the repulsive exchange repulsion due to the Pauli principle. Consequently, the dispersion is essentially a correlation effect, and it belongs to the most difficult cases for accurate description by the basis set quantum chemical approaches. The mentioned four components are well-defined within the framework of symmetry-adapted perturbation theory (SAPT,²² for more details see below) and provide a solid and insightful background for analysis of intermolecular interactions.²¹ Note, however, that most benchmark quantum chemistry methods provide only the total interaction energies, and it is difficult to decompose them to the mentioned basic components.

One of the especially important directions is the chemistry of large systems with noncovalently interacting constituents such as biomolecular complexes,²³ host-guest complexes,^{24–26} molecule-surface interactions,^{27–29} or behavior of large molecular ensembles.^{30,31} These applications motivate the development of scalable and robust computational methods^{32–36} that can simulate complex processes for large numbers of atoms. These methods typically rely on approximations that are parametrized either by using experimental data, or, more recently, by reference quality calculations.

1.1. Benchmark Calculations

After several decades of effort, reference quantum mechanical calculations are capable of providing highly accurate and reliable predictions. Such computational studies play an important role in theoretical modeling,^{37,38} essentially for two reasons. First, they allow for accurate predictions whenever experimental data is not available. Second, reference results are highly valuable for calibration and parametrization of computational methods which enable studies of large systems that are crucial for application areas. Examples include developments of new exchange-correlation functionals in density functional theory (DFT),³⁹ semiempirical methods,⁴⁰ or model potentials/force fields for molecular mechanics.^{41,42} What are the accuracy requirements for the benchmark calculations of intermolecular interactions? As a minimum requirement, the chemical accuracy of 1 kcal/mol is often mentioned as an important criterion for accurate predictions of thermochemical processes. However, this threshold appears as being too loose for complexes bound by fractions of kcal/mol where an error of 1 kcal/mol can be overwhelming. For small complexes bonded by dispersive interactions, we therefore adopt the subchemical accuracy of 0.1 kcal/mol⁴³ as much more appropriate. We note that the

relative error measure is useful to assess errors for different types of complexes on equal footing.^{44,45}

Technically, interaction energies in molecular complexes are usually calculated using the so-called supermolecular approach, where interaction energy is calculated as a difference between total electronic energies of the molecular complex and its constituents. In an alternative approach, intermolecular perturbation theory, the interaction energy components are calculated directly, without the need to evaluate comparatively large total electronic energies. The latter approach is less common but very important. It should be noted that most benchmark calculations on complexes composed of light elements do not include relativistic effects⁴⁶ due to their small contributions to these interactions.⁴⁴

The supermolecular approach requires calculations of very accurate total electronic energies of atoms and molecules. Quantum chemistry offers a plethora of methods at varying levels of approximation, from very approximate empirical and semi-empirical ones through quite accurate DFT methods to very accurate approaches that include, for example, many-body wave function theory (WFT), perturbation theories, or quantum Monte Carlo (QMC). Accuracy is essential especially for weak intermolecular interactions where a subtle balance in bonding results from the long-range dynamical correlations (dispersion). For instance, a number of recently introduced DFT functionals have been designed to describe the long-range correlations. Although empirically or theoretically derived DFT corrections improve the description of dispersion effects quite significantly, they are not guaranteed to provide systematic benchmark quality results due to their empirical nature. Another possibility is offered by perturbation approaches, such as MP2, MP3, etc., that represent another class of quantum mechanical methods that are very popular and powerful. Although these methods naturally include dispersion effects, they often show systematic errors that cause disbalance of various contributions to intermolecular interactions, so that the overall accuracy at the MP2 level is not guaranteed in general. In addition, convergence in perturbation order can be very slow. Therefore, many of the commonly used methods are simply not accurate enough whenever high accuracy is the key requirement as is almost invariably the case for noncovalent interactions.

The most accurate and reliable results are obtained from traditional and well-established methods of WFT. The electron-electron correlations are introduced through the expansion of the many-body wave function using singly (S), doubly (D), triply (T), etc. excited determinants from the reference wave function. The rapidly growing number of such terms with the excitation level is an obvious source of exceedingly steep growth of computational cost with the increase in accuracy. When all excited determinants are included, as in the full configuration interaction (FCI) method, one obtains the best variational result within the given basis set. Due to the exponential scaling with the number of electrons and basis functions, FCI calculations can be performed only for small systems consisting of a few atoms.

Over time, the coupled cluster (CC) approach^{47–49} emerged as the most practical WFT reference method, and CC with singles, doubles, and perturbative triples CCSD(T)^{44,50–58} is often considered a “gold standard” for many applications including intermolecular interactions. We note that accuracy of CCSD(T) has not yet been confirmed in large molecules and uncertainties regarding its accuracy may need adjustments of conclusions drawn for the benchmarks performed today. The computational cost of CC methods like CCSD and CCSDT

scales as $O(K^6)$ and $O(K^8)$, respectively, where K is the basis set size so that it is applicable to small and medium size systems. In favor of the WFT as a benchmark quality approach speaks the very extensive experience with these methods and the fact that they allow for systematic improvements both by increasing the size of one-electron (atomic) basis sets and by increasing the level of excitations.

Comparisons of FCI and CC methods for small complexes where FCI calculations are viable show that CC theories have turned out to be very reliable, provided that triple excitations are included at least at the CCSD(T) level⁵⁹ and the wave functions do not exhibit significant multireference effects. So far for slightly larger complexes, the only practical cross-check is comparison of calculations with increasing levels of theory, such as CCSDT, CCSDT(Q), and CCSDTQ.^{44,58–61} From these studies, it appears that CCSD(T) extrapolated to the complete basis set (CBS) limit, CCSD(T)/CBS, is indeed a very accurate method for intermolecular interaction energies and very likely it provides results beyond chemical accuracy of 1 kcal/mol, at least for the complexes where higher level calculations were viable. Thus, CCSD(T)/CBS is among the most trusted and widely applied methods for accurate calculations of noncovalent interactions.^{13,37,62}

Additional support for quality and accuracy of the CCSD(T) results came from a different branch of WFT methods: the intermolecular perturbation theory. In particular, SAPT^{22,63} is a method that focuses on a direct evaluation of the intermolecular interactions, without the need to calculate total energies of the monomers and the noncovalent complex. Most current applications use computationally more efficient DFT-based SAPT decomposition schemes, SAPT(DFT)⁶⁴ or DFT-SAPT.⁶⁵ Many favorable comparisons of the intermolecular perturbation results with the supermolecular calculations have been published, and we refer the interested reader for instance to a recent paper comparing SAPT and CCSD(T) results for the S22⁵⁴ set of molecular complexes.⁶² The fact that these alternatives and largely independent sources of reference data show very good agreement is quite important and increases the confidence in quality of the reference interaction energies. In this respect, it is particularly promising that QMC, which is methodologically a very different approach, is also able to provide results in agreement with CCSD(T) within the criteria of subchemical accuracy.^{58,66–68}

Unfortunately, wave function based methods have several well-known limitations. One of them is particularly slow convergence of the correlation energy with the size of the atomic (one-particle) basis set. Resulting basis set incompleteness and basis set superposition errors are fairly large for commonly used bases (e.g., of triple- ζ quality). Much larger basis sets, preferably augmented with diffuse basis functions are necessary for benchmark calculations. Multiple composite methods have been suggested for thermochemistry (see, e.g., ref 69) and later used in biomolecular interactions⁷⁰ to mitigate this problem. In general, they combine CBS extrapolation at a lower (less demanding) level of theory with evaluation of the higher-order correlation effects (typically triple or quadruple excitations) in a smaller basis set. Since the energy differences converge more progressively than the total energies, one would expect that smaller bases in combination with CBS extrapolation schemes would suffice. However, methods that guarantee generally transferable energy differences in noncovalent complexes require limiting basis set sizes at the CC level, of the order of augmented double/triple- ζ quality.^{13,60,71} Consider-

ing such framework, these methods are therefore still considerably computationally demanding and exhibit very unfavorable scaling with the system size. Among the largest calculated complexes is, for instance, coronene dimer.⁷² Although linear scaling methods are being introduced,^{73–75} additional testing may be necessary to map out the areas and limits of their applicability. Another problem of wave function theories is the treatment of complexes with partially multireference character. The gold standard CCSD(T) method is meant primarily for systems with minimal contribution of static correlations. The multireference CC methods are still under development,^{76,77} similarly to other branches of multireference wave function theories, and in general, they are not ready to be used as black-box methods for benchmarking purposes. Finally, CC approaches are not easily implemented for periodic systems (crystals, surfaces, or liquids). As we discuss below, QMC methods offer an important advantage in comparison with the wave function methods in some of these problematic cases.

1.2. Why Quantum Monte Carlo?

Electronic structure quantum QMC is a set of methods for solving the stationary Schrödinger equation based on stochastic techniques such as use of stochastic processes and sampling of wave functions in the space of electron positions. Due to its favorable properties, QMC has made inroads into several areas of electronic structure theory, in particular, into those where the electron correlation is an important or dominant issue.

The results obtained over the past two decades show that QMC is becoming a valuable and effective methodology, especially in regard to challenges posed by noncovalent interactions. Initially, it was not at all obvious that for systems with dispersive interactions QMC could provide new insights or be competitive. However, as the QMC calculations have become more systematic, it turned out that for a number of important noncovalent systems, it has reached the accuracy that is approaching the desired benchmark quality. This can be seen on calculations of small complexes with comparisons of projector QMC versus CCSD(T)^{66–68,78,79} and CCSDT(Q).⁵⁸

Equally important have been new insights into the electronic structure of noncovalently interacting systems with regard to the choice of appropriate trial wave functions and corresponding biases from QMC approximations such as the fixed-node error.^{66,80–82} In addition, QMC has allowed calculations of much larger complexes than are feasible within mainstream wave function methods in quantum chemistry (e.g., refs 83 and 84). These results suggest that QMC provides a new alternative for studies that aspire to overcome the current limits of accuracy or sizes that are needed for studies of systems such as molecules on crystal surfaces²¹² or layered two-dimensional (2D) materials.^{159,214,247}

We would also like to note that QMC and current mainstream correlated WFT methods appear to be rather complementary to each other. At the qualitative level, one can identify several reasons why. Traditional correlated methods depend very significantly on the size of the basis sets, while QMC results are much less sensitive to this aspect. Basis set methods are very inefficient in treating the so-called dynamical correlation, while in QMC this is rather straightforward to capture. It is easier to implement QMC on parallel architectures and apply to larger systems while there are significant obstacles to do so for basis set correlated approaches. QMC also allows treatment of periodic systems and/or systems with multireference character (by employing multireference trial wave functions). On the other

hand, unlike in traditional methods, QMC has its own difficulties such as the Fermion sign problem or inefficiencies from large energies of atomic cores that force the use of effective core potentials.

1.3. Review Scope

The current review is intended to provide a comprehensive state-of-the-art picture of electronic structure QMC, its technical aspects, and its applications to systems with noncovalent interactions. We outline only the most used electronic structure QMC methods; however, for more exhaustive covering of various details, we refer to a number of previously published reviews, introductory texts, and tutorials.^{85–99} We also do not attempt to review methods for problems that involve quantum treatment of nuclei.^{98,100–107,110,111}

The review begins with a general introduction to QMC methods (section 2) and continues with the discussion of its specifics for noncovalent interactions and related literature review of practical aspects relevant in applications (section 3). Applications of QMC to a variety of systems with noncovalent interactions (section 4) are sorted according to criteria relevant to areas of interest such as materials science, chemistry, and physics. The final section is devoted to extensive discussion of open challenges (section 5).

2. QUANTUM MONTE CARLO (QMC)

Already in the 1930s, E. Schrödinger and E. Fermi pointed out the similarities between the Schrödinger equation in imaginary time and the diffusion equation. This correspondence was very suggestive and indeed the first attempts to use a stochastic diffusion-like process to solve the Schrödinger equation date back to the first computational simulations of physical systems established during the Manhattan Project. The idea became practical with the advent of mainframe computers and later it has evolved into a family of methods broadly known as quantum Monte Carlo (see, for example, refs 89 and 95 and refs therein). Over the past three decades, it has been further extended to both discrete and continuous systems and applied to a great many systems described by variety of Hamiltonians and various settings in nuclear physics, condensed matter physics, quantum chemistry, etc. This should not be surprising since the stochastic methodologies have a number of attractive properties: (i) direct and accurate description of particle correlations; (ii) favorable scaling when compared with other correlated wave function methods; (iii) wide range of physical/chemical effects and mechanisms which can be studied such as bonding/cohesion, optical properties, many-body properties, etc. in molecules, solids, or appropriate models; (iv) scalability on parallel and distributed architectures, including the largest massively parallel machines; and (v) history of important benchmarks such as the correlation energy of electron gas¹⁰⁸ that have been widely used in DFT functionals.

Further benchmarks include calculations of He quantum liquids,¹⁰⁹ Bertsch parameter for Fermions at unitarity,¹¹² and a number of other systems.

This part continues with the description of projector QMC and introduces perhaps the most commonly used diffusion Monte Carlo (DMC) method with the fixed-node (FN) approximation. Since the quality of FNDMC results relies on quality of trial wave functions, we introduce their most frequently used forms (section 2.2) and strategies for variational optimizations (section 2.3) by virtue of the variational Monte Carlo (VMC) method. Subsequently, we discuss effective core

potentials (section 2.4) important in QMC to reduce computational demands, treatment of periodicity (section 2.5), limitations of QMC and its CPU cost scaling (section 2.6), and finally, we cover the practical QMC workflow (section 2.7).

The projector QMC methods are based on the following equation

$$\Psi_0 = \lim_{\tau \rightarrow \infty} \exp[-\tau(H - E_T)]\Psi_T \quad (1)$$

where Ψ_0 is the ground state with desired symmetries, τ is a real parameter (imaginary time), H is the Hamiltonian, and Ψ_T is the initial trial (or variational) wave function. E_T is an energy offset that keeps the normalization of Ψ_T asymptotically constant. The stochasticity comes into play as a method of solving this equation as well as a way of calculating the expectation values. In particular, in the variational Monte Carlo (VMC) one estimates expectations, such as the variational energy, in a statistical manner. The variational energy can be rewritten as an average of the local energy $[H\Psi_T]/\Psi_T$ samples with a statistical uncertainty ϵ_{stat}

$$\begin{aligned} E_{\text{var}} &= \frac{\langle \Psi_T | H | \Psi_T \rangle}{\langle \Psi_T | \Psi_T \rangle} = \frac{\int |\Psi_T|^2 [H\Psi_T] / \Psi_T d\mathbf{R}}{\int |\Psi_T|^2 d\mathbf{R}} \\ &= \frac{1}{M} \sum_{m=1}^M \frac{[H\Psi_T(\mathbf{R}_m)]}{\Psi_T(\mathbf{R}_m)} + \frac{\text{const}}{\sqrt{M}} = E_{\text{VMC}} + \epsilon_{\text{stat}} \end{aligned} \quad (2)$$

where $\mathbf{R} = (\mathbf{r}_1, \dots, \mathbf{r}_N)$, while N is the number of electrons. The set of random samples $\{\mathbf{R}_m\}_{m=1}^M$ of particle positions is distributed according to $|\Psi_T|^2$. These samples are often colloquially called random walkers, see Figure 1, top and middle. Since the particle positions are eigenstates of the position operator, QMC has the important property that it a priori samples from the complete basis. In addition, the extent of sampling is automatically adjusted so that the stochastic error bar, that scales with $M^{-1/2}$, is below the desired threshold. This is one of the key differences with almost all correlated wave function methods that rely on (or suffer from) finite basis sets used to describe the eigenstates. We note that the question of basis sets will enter the QMC picture, but its role there is rather different and its impact is much more diminished as explained later. An example that illustrates the total energy convergence of projector QMC versus CCSD(T) methods with respect to the one-particle basis set size is given in Figure 2. Clearly, the correlation energy calculated using the real-space walks (complete basis) and nodal boundaries converge very rapidly, although the total energy differences may suffer from biases (from various approximations) that must be carefully controlled, as we explain later.

2.1. Diffusion Monte Carlo for Electrons

The action of $\exp[-\tau(H-E_T)]$ on the wave function (eq 1) can be rewritten as the Schrödinger equation (a.u.) in imaginary time

$$\partial_\tau \Psi(\mathbf{R}, \tau) = [(1/2)\nabla_{\mathbf{R}}^2 - (V - E_T)]\Psi(\mathbf{R}, \tau) \quad (3)$$

that resembles the diffusion equation with the additional rate (or branching) term $(V-E_T)$. One can imagine Ψ as an ensemble of Brownian particle(s) diffusing in the configuration space with the rate of disappearance or proliferation driven by the potential term (Figure 3), while E_T is adjusted to keep the number of walkers to be, on average, constant. It is convenient to recast eq 3 into an integral form

$$\Psi(\mathbf{R}, \tau + \Delta\tau) = \int G(\mathbf{R}, \mathbf{R}', \Delta\tau)\Psi(\mathbf{R}', \tau) d\mathbf{R}' \quad (4)$$

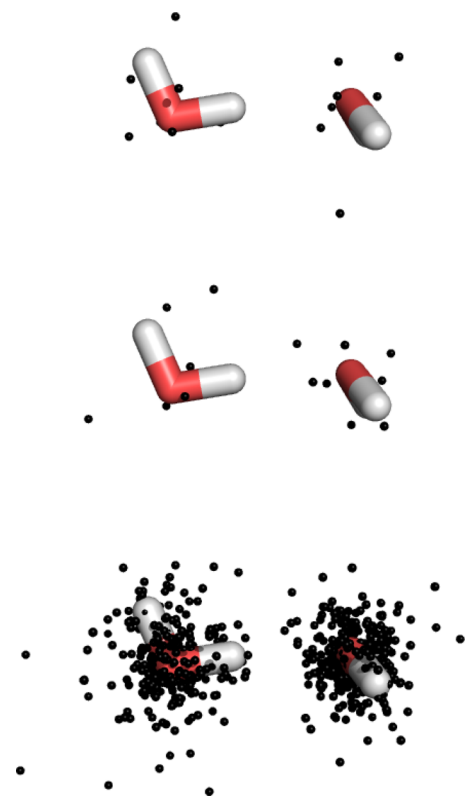


Figure 1. Two representative snapshots (top and middle) of random walkers in the position space of electron configurations from a QMC simulation of the water dimer. Statistically, the wave function is represented by the density (histogram) of the accumulated walker ensemble (bottom).

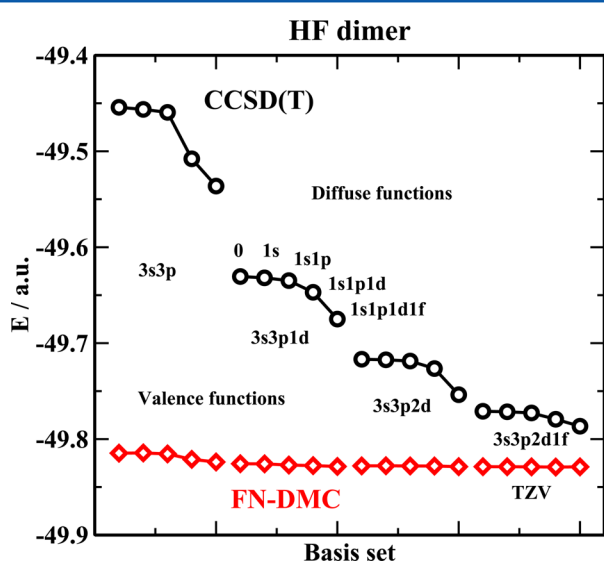


Figure 2. Dependence of CCSD(T) and FNDMC total energies on the one-particle basis set saturation for the HF dimer. The employed basis sets consist of valence and diffuse functions as indicated. Note the very mildly varying FNDMC energy with the increasing basis set level. The FNDMC method depends on the basis set only indirectly, through the construction of Ψ_T .

By interpreting the Green's function $G(\mathbf{R}, \mathbf{R}', \Delta\tau) = \langle \mathbf{R} | \exp[-\Delta\tau(H - E_T)] | \mathbf{R}' \rangle$ as a transition probability for propagating the quantum amplitude from $\mathbf{R}' \rightarrow \mathbf{R}$, it becomes rather natural to represent the wave function (Figure 1, bottom) as a set of

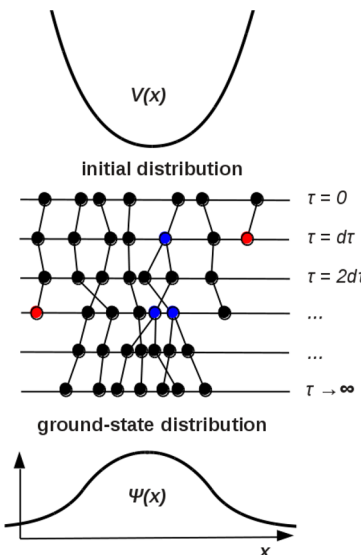


Figure 3. Illustration of a toy DMC algorithm for a one-dimensional attractive potential $V(x)$. The samples are initialized from a uniform distribution over a finite interval. The imaginary time τ propagation of walkers consists of diffusion and branching. The branching causes that walkers to disappear (die) in the regions of high potential energy (red) and to multiplicate in the low-energy region near the potential minimum (blue). In the limit of infinite time, the distribution samples the exact ground state $\Psi(x)$.

random points (walkers, Figure 1, top and middle panels) evolving in the space of configurations, i.e.,

$$\Psi(\mathbf{R}, \tau) = \text{hist}\left[\sum_m^M \delta[\mathbf{R} - \mathbf{R}_m(\tau)]\right] + O(1/\sqrt{M})$$

where the function “hist” denotes a histogram with an appropriate resolution. The Green's function $G(\mathbf{R}, \mathbf{R}', \Delta\tau)$ can be approximated for $\Delta\tau \rightarrow 0$ by the Trotter expansion, and consequently, eq 4 can be solved by iterations, effectively reaching the large projection time. The time step bias is of the order $O(\Delta\tau^n)$, where $n = 2-3$ and, it is straightforward to make it small by extrapolations to $\Delta\tau \rightarrow 0$.¹¹³

Up to this point, we did not consider the fact that for many-Fermion systems, the quantum amplitudes are both positive and negative, while in the presence of currents, the amplitudes are inherently complex. Unfortunately, this leads to the infamous Fermion sign problem: it is not too difficult to show that the antisymmetric amplitudes make the described algorithm inefficient and its cost growing exponentially with the system size and/or desired accuracy.^{89,91} One of the ways to address this complication is to make the sampled distribution positive definite. Let us assume that Ψ_T is the best available approximation for a Fermion ground state Ψ_0 (for simplicity we assume that these states are real). The Fermionic state exhibits the so-called node (i.e., zero locus of the wave function that is defined as $\Gamma = \{\mathbf{R}; \Psi_T(\mathbf{R}) = 0\}$). The node Γ is a subset of configurations for which the wave function vanishes, and for N Fermions in three-dimensional (3D) space it is, in general, a $(3N-1)$ -dimensional hypersurface that divides the configurations into domains with positive and negative wave function values. If we require the node of the solution Ψ in eq 4 to be the same as the node of Ψ_T then the domains of these two wave functions will have the same sign structure. On the basis of this

boundary condition, we can form the product distribution $f = \Psi\Psi_T$ that obeys

$$f(\mathbf{R}, \tau) = \Psi(\mathbf{R}, \tau)\Psi_T(\mathbf{R}) \geq 0 \quad (5)$$

for any τ . Imposing this boundary condition (see Figure 4 for illustration) is known as the fixed-node approximation, and the

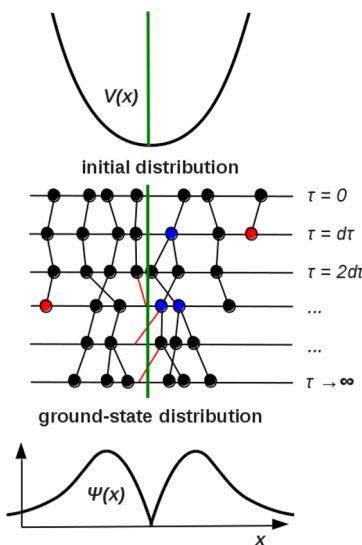


Figure 4. Illustration of a toy FNDMC algorithm in a one-dimensional attractive potential $V(x)$. The samples are initially drawn from a uniform distribution. The imaginary-time τ propagation consists of diffusion, restriction of node-crossing, and branching. In the limit of infinite time, the distribution samples the exact ground state $\Psi(x)$ within the constraint imposed by the node, where the potential barrier is infinite. The node therefore enforces $\Psi(x)$ to sample an excited state.

related method is known as the fixed-node diffusion Monte Carlo, denoted as FNDMC from now on. It is straightforward to show that for local (i.e., multiplicative) potentials, it produces an upper bound for the energy.¹¹⁴ For complex wave functions, the analogous condition can be formulated as a fixed-phase approximation.¹¹⁵

Apart from the Fermion sign problem, the basic DMC algorithm introduced above suffers from the poor statistical error convergence that can be significantly improved by the importance sampling transformation.¹¹⁶ The fixed-node condition and importance sampling are both conveniently obtained by simulating a master equation for the product distribution $f(\mathbf{R}, \tau)$, obtained from the original evolution eq 3 multiplied by Ψ_T , that reads

$$\partial f = (1/2)\nabla^2 f - \nabla \times (f \nabla \ln |\Psi_T|) - (E_{\text{loc}} - E_T)f \quad (6)$$

where $E_{\text{loc}} = [H\Psi_T]/\Psi_T$, with the corresponding rearrangements of the integral form (eq 4). Besides the diffusion term, the resulting second-order operator exhibits also a new drift term and the potential energy is replaced by the local energy. The drift vector $\nabla \ln |\Psi_T|$ points toward the regions of the configuration space where Ψ_T amplitudes are large. Since it diverges at the node, it forbids the node crossing, imposing thus the fixed-node condition. Note that by this transformation the large fluctuations from the potential energy are replaced by much smaller fluctuations of the local energy. This results in a very substantial improvement of the overall efficiency, often by orders of magnitude, depending on the quality of Ψ_T .

Clearly, the Fermion sign problem forces us to make a nontrivial departure from the formally exact projection formulation, and the fixed-node approximation, in general, leads to some systematic bias. Unlike the one-particle basis set biases in the mainstream methods that have been studied for many decades, the nature of the fixed-node bias is, at least initially, somewhat nebulous. In order to shed some light on it, one can show that the convergence to the exact energy scales quadratically in the nodal displacement error.⁸⁹ Consequently, the knowledge of the exact node would enable recovery of the exact eigenvalue (in polynomial time), and the fixed-node algorithm would produce samples of the exact eigenstate. Of course, what is crucial for practical applications is the total error and that includes not only scaling but also the prefactor. It is quite challenging to find a rigorous bound for the prefactor, and therefore, the estimates mostly rely on *a posteriori* assessments. There is a substantial body of electronic structure FNDMC calculations that show that the fixed-node bias is rather small, one can perhaps even say, unexpectedly small. For the total energies, even when using just single-reference trial wave functions such as the ones based on HF orbitals, the error is typically not bigger than 5–10% of the correlation energy ($E_{\text{corr}} = E_{\text{exact}} - E_{\text{HF}}$). This value is sufficient for predictive energy differences such as cohesion, bonding, excitations, etc., often within a few percent of the experiments. Systematically improved multideterminant wave functions were shown to achieve near chemical accuracy (1.2 kcal/mol in average) for atomization energies.¹¹⁷ For large systems, this approach might be too demanding in general. However, a few determinant trial functions that describe, say, excited singlets in gap calculations of supercell solids are feasible. In small molecular systems, on the other hand, the CC methodology provides accurate answers for lower cost. For noncovalent interactions, the fixed-node bias is especially relevant and it is very favorable that in these types of systems it largely cancels out. We further focus on this particular aspect in some detail later (section 3.2). Although the nodes are systematically improvable, so far the cost of such improvements is significant. Nevertheless, some progress in understanding the nodal properties and their impact on calculated energies has been achieved over the last three decades.^{118–122} Before we go any further into the fine points of the fixed-node errors, let us first introduce the trial wave functions that are commonly used in FNDMC calculations.

2.2. Trial Wave Functions

Another important advantage of stochastic methods is the vastly increased variational freedom for capturing the many-body effects explicitly. The random sampling not only enables the exploration of much larger space of suitable functional forms but also can lead to much more compact wave functions. For example, it is straightforward to capture the leading nonanalytical behavior such as electron–nucleus and electron–electron cusps explicitly and exactly. Clearly, this recovers a significant part of the correlations that are otherwise difficult to describe in methods that are built upon one-particle bases.

The most widely used forms are the Slater-Jastrow trial wave functions with an antisymmetric part Ψ_A given by single- or multireference Slater determinant(s) multiplied by a symmetric positive definite Jastrow-Bijl correlation factor J

$$\begin{aligned} \Psi_T = \Psi_A \times J &= \sum_n c_n \det_n^\dagger [\varphi_k^\alpha(i)] \det_n^\dagger [\varphi_l^\beta(j)] \\ &\times \exp(U_1 + U_2 + U_3 + \dots) \end{aligned} \quad (7)$$

where $\{\varphi_k^\alpha\}$, $\{\varphi_l^\beta\}$ are single-particle orbitals, and U_i are functions that describe the correlations. The one-particle orbitals are typically obtained from self-consistent methods such as HF, DFT, and GVB or as natural orbitals from configuration interaction (CI) or other correlated approaches which enable explicit construction of Ψ_T . The orbitals are most often represented by commonly used Gaussian basis sets, although QMC can easily accommodate also Slater, numerical, plane wave, etc., bases as well as their mixtures. The correlation factor describes the particle correlations explicitly and is very effective in capturing a large part of the correlation energy at low cost. The commonly used forms for correlation functions depend on electron–electron (r_{ij}) and electron–nucleus (r_{il}) distances

$$U_1 = \sum_{i,j} u_{el}(r_{ij})$$

$$U_2 = \sum_{i,j} u_{ee}(r_{ij}) + \sum_{i,j} u_{el}(r_{ij}, r_{il})$$

$$U_3 = \sum_{i,j,l} u_{ee}(r_{ij}, r_{il}, r_{jl}) + \dots$$

although more general forms that depend on \mathbf{r}_{ij} , \mathbf{r}_{il} , etc., have been explored.¹²³ U_1 affects only one-particle density and can be absorbed into the one-particle orbitals; however, it is more convenient to keep it in the Jastrow factor so that the density can adjust to the impact of higher-order terms during the optimization. The correlation functions u are expanded in appropriate basis sets such as Padé polynomials⁹¹ or similar smooth functions that saturate to a constant at large distances. Note that the explicit electron–electron correlation enables one to describe the corresponding cusps in the wave functions exactly. The correlation functions contain typically from a few to a few tens of expansion parameters that are optimized variationally, as explained in more detail in the following section 2.3.

There are other choices for the trial functions, some of them rather sophisticated and designed to describe particular aspects of many-body correlations. For description of quantum condensates with pairing but also for electronic structure in general, the pair orbital Bardeen-Cooper-Schrieffer¹²⁴ and pfaffian¹²⁵ wave functions were successfully applied to several types of systems. Another form generalizes the Slater determinant with collective backflow coordinates^{126,127} that have been inspired by insights into the behavior of quantum liquids.

2.3. Optimization of Trial Wave Functions

The trial wave functions contain parameters that can be optimized using the stochastic estimations for the variational energy or the local energy variance

$$\sigma_E = \langle ([H\Psi_T]/\Psi_T - E_{VMC})^2 \rangle_{\Psi_T^2} \quad (8)$$

using the VMC samples. These optimizations are quite involved due to the statistical noise that hinders calculations of gradients or Hessians and therefore require specially adapted methods. For example, a minimization of the variational energy for a given VMC sample set could be unstable for particular values of parameters since the sampling for many-electron systems is always very sparse. That is also one of the motivations why variance is often employed to make the optimization more robust since it is always bounded from below.¹²⁸ Therefore, the most commonly used cost or objective functions are weighted

combinations of energy and variance.¹²⁹ A number of methods has been developed over the years that apply sophisticated techniques for filtering out the noise and lead to robust algorithms that optimize the parameter sets more efficiently.^{129–132} Besides the energy, variance and their linear combinations, other cost functions such as

$$\sigma_E = \langle |[H\Psi_T]/\Psi_T - E_{VMC}| \rangle_{\Psi_T^2} \quad (9)$$

have been used since the absolute value diminishes the impact of large energy fluctuations from samples that are, for example, close to the nodes where the local energy typically diverges. Note that the local energy distribution is generically non-Gaussian and exhibits heavy tails¹³³ that add to the optimization difficulties.

There are several types of parameters that can be optimized: (i) parameters in the Jastrow functions, (ii) coefficients of multireference expansions, (iii) one-particle orbitals, (iv) and possibly other, more complicated terms such as backflow^{126,127} or pair orbitals.^{124,134}

Although the multireference expansion coefficients and orbitals are optimal within the used self-consistent method, the presence of Jastrow functions has a significant impact on these. In particular, the reoptimization of expansion coefficients often improves the wave functions quite substantially as has been shown by Umrigar and co-workers.¹²⁹ The effect of orbital reoptimization can vary from small to notable, depending on the type of application.

Another approach that has proved to be useful is the improvement of the wave function indirectly, through the optimization of an effective Hamiltonian that is used in the theory that generates the orbitals.¹³⁵ For example, consider a hybrid DFT functional with the weight of exact exchange denoted as w . For a given value of w , one obtains a set of orbitals $\{\varphi_i(\mathbf{r};w)\}$ that is used to construct the trial function $\Psi_T(\mathbf{R};w)$ and subsequently to evaluate the fixed-node energy $E_{FNDMC}(w)$. By appropriate scanning of the weight, one can find the optimal w that provides the lowest fixed-node energy. The approach has been successfully applied to transition metal oxygen, and other systems,^{135–137} and it turned out that the optimal percentage is in the range of 10–30%, with the region around the minimum being rather shallow. Note that this provides not only the variationally improved trial wave function (and nodes), but it also generates the optimal effective Hamiltonian within the given theory. It is worth mentioning that these results have confirmed that the value of $w = 0.25$ (or similar) in B3LYP and some other hybrid DFT functionals are close to the optimal one found by the variational, many-body QMC approach. The agreement is remarkable since B3LYP functional, for example, was based on a fit for first- and second-row molecules, while the mentioned applications were mostly focused on strongly correlated molecular and solid systems with transition metals.

2.4. Effective Core Potentials

The computational demands of QMC methods are determined by the dominant energy fluctuations encountered in the statistical sampling. Since the energies of core states grow as Z^2 , where Z is the atomic number, the core degrees of freedom are very costly and overall demands are proportional to $\approx Z^p$ where the exponent $p \approx 6$. In addition, in calculations that contain core states most of the computational time is used on averaging out large fluctuations of kinetic and potential energies around the nucleus, although for most valence properties, these have negligible impact. A few decades back, it has been recognized that atomic core states can be replaced by the

effective core potentials (ECPs) or pseudopotentials (as they are called in condensed matter physics) that mimic as closely as possible the impact of the removed core electrons on the valence states. Especially for heavier atoms, the valence-only settings with ECPs are often used to simplify and speed-up the calculations even in cases when frozen cores can be used. Although ECPs can introduce biases, for most of the valence properties, one can verify that such biases do not affect the desired properties within the given accuracy. The accuracy of ECPs can be systematically increased, for example, by taking more core electrons into the valence space or by more accurate constructions. Further corrections such as polarizability and core relaxation effects can be captured as well by additional terms.¹³⁸ ECPs, besides complications from the nonlocal projectors, also have advantages since they enable the inclusion of the relativistic effects, both scalar and also spin–orbit for heavier elements.

There exists a plethora of ECPs/pseudopotentials forms, but the most commonly used one is a sum of two terms: a local radial part that at large distances behaves as the Coulomb potential with effective valence charge, Z_{val}/r , and the nonlocal part. For the nonlocal component, we consider only the simplest semilocal version that is given by

$$W_J = \sum_l^{l_{\max}} v_l(r_j) \sum_m |Y_{lm}\rangle \langle Y_{lm}| \quad (10)$$

where v_l is the radial pseudopotential function, and for simplicity, we assume a single (pseudo) ion J located at the origin. The ECP operator is local in the radial distance from the ion, while it is nonlocal in the corresponding angular variables. The summation over l typically includes a few lowest angular momentum channels.

Although ECPs increase the efficiency by orders of magnitude, they also complicate the DMC calculations quite significantly. The reason is that the projectors can produce negative Green's function matrix elements (i.e., they can create another type of a sign problem that has to be avoided). This problem is straightforward to understand from the expression for the matrix element

$$\langle \mathbf{R} | W | \mathbf{R}' \rangle = \sum_{j,i,l} \frac{2l+1}{4\pi} v_l(r_{ij}) \frac{\delta(r_{ij} - r'_{ij})}{r_{ij}^2} P_l(\hat{\mathbf{r}}_{ij} \cdot \hat{\mathbf{r}}'_{ij}) \quad (11)$$

where P_l is the l th Legendre polynomial and $\hat{\mathbf{r}}_{ij}$, $\hat{\mathbf{r}}'_{ij}$ are unit vectors in corresponding directions. It is clear that the nonlocality (i.e., nonzero matrix elements between different primed and unprimed angles) can lead to appearance of negative probabilities in a walker's evolution.¹³⁹ Note that this is unrelated to antisymmetry since the negative signs here can appear even for a single-electron problem.

Approaches to avoid this difficulty have been developed some time ago.^{140–142} In the localization approximation,¹⁴² the nonlocal part of the ECP is projected onto the best available Ψ_T as

$$W_{\text{eff}} = \Psi_T^{-1}(\mathbf{R}) \int \langle \mathbf{R} | W | \mathbf{R}' \rangle \Psi_T(\mathbf{R}') d\mathbf{R}' \quad (12)$$

This results in an effective, local, many-body potential that replaces the nonlocal operator W . However, W_{eff} depends on the trial function, and therefore, the variational property with regard to the original Hamiltonian is not guaranteed. On the other hand, as we have shown elsewhere,¹⁴² the localization bias in energy scales quadratically in the error of Ψ_T and therefore, for accurate

trial wave functions, this provides a practical way to carry out the calculations. More details on this aspect can be found elsewhere.^{89,143} Note that the localization error is difficult to disentangle from the fixed-node bias since the nodal error distorts the wave function also elsewhere and therefore does affect the projection as well. Typically, for small-core ECPs, the localization error is often smaller or comparable to the fixed-node error, although this is not automatically guaranteed for very heavy atoms with large repulsive potential functions that have a sizable radial extent. Recent results suggest that more research is needed to both improve ECPs and their treatment in QMC for heavy atoms.

In order to preserve the variational property for the original Hamiltonian with W , more elaborate methods for treating the ECPs have been proposed. This involves explicit sampling of the nonlocal operator matrix elements for paths that do not generate negative signs while using the localization projection for the part that does.¹⁴⁴ In the DMC method, this algorithm goes under the name of T-moves as it was introduced by Casula.¹⁴⁵

2.5. Treatment of Periodicity

QMC methods can be applied to molecules with free-boundary conditions but also to periodic systems with one-, two-, and three-dimensional periodicity. This allows for calculations of crystals, surfaces, or atomic and molecular wires. For these applications, QMC has a unique position in providing many-body, high-accuracy results that are very difficult to obtain by other correlated wave function methods. We briefly mention the main features of such calculations since van der Waals crystals, adsorption of molecules on surfaces, graphene or graphene-like layered 2D materials are of high interest for many application areas (see section 4).

In QMC, the periodicity is accommodated by simulating a supercell with periodic boundary conditions. Typically, calculations with several supercell sizes are performed and followed by extrapolations to the thermodynamic limit. Clearly, periodicity adds complications to the evaluation of the long-range Coulomb interactions. The resulting total Coulomb energy involves contributions within the supercell as well as interactions with the periodic array of supercells (images) so that the total potential energy with charges $\{q_i\}$ is given

$$V_{\text{scell}} = \frac{1}{2} \sum'_{i,j} \sum_{\mathbf{R}_s} \frac{q_i q_j}{|\mathbf{r}_i - \mathbf{r}_j - \mathbf{R}_s|} \quad (13)$$

where \mathbf{R}_s are lattice vectors of the supercell lattice and the prime indicates that the term with $i = j$ is omitted when $\mathbf{R}_s = \mathbf{0}$. Tacitly, we assume that the system is neutral so that $\sum_i q_i = 0$. The sum is conditionally convergent and depends also on boundaries so that appropriate analytical considerations are necessary for physically meaningful results. One possible solution is the Ewald construction of adding spherical shells that leads to a finite and explicit expression for the potential energy

$$V_{\text{scell}} = \sum_{i,j} q_i q_j v_{\text{ew}}(\mathbf{r}_i - \mathbf{r}_j) + e_s \quad (14)$$

where v_{ew} is the resulting Ewald (periodic Coulomb) interaction and e_s is a constant (see, for example, ref 89). Analysis of the Ewald contributions shows that the leading term in the finite size bias scales as $1/N$, where N is the number of electrons in the supercell.⁸⁹ The prefactor of this bias can be decreased very significantly by appropriate modifications, for example, using the

model periodic Coulomb interaction that was derived and tested by Foulkes and collaborators.^{146–148}

There is another source of the finite size bias that comes from the kinetic energy, since for a typical supercell size only a sparse set of k-points in the Brillouin zone is sampled. Application of the so-called twisted boundary conditions (twist-averaging), where one samples over different k-points by independent calculations significantly diminishes the impact of this contribution. Both of these finite size biases are proportional to the inverse supercell volume, and therefore, the thermodynamical limit is obtained by extrapolation using data from several supercell sizes. The very recent benchmarking study presents a comprehensive set of corrections that significantly minimizes the biases and speeds-up the convergence.¹⁴⁸

For insulators, it is straightforward to estimate the thermodynamic limit by reaching supercells with a few tens of atoms, and calculations have been carried out for a range of solid systems.^{93,149} For metals, the problem can be more involved, depending on the shape and topology of the Fermi surface. In particular, the supercell should be large enough so that occupied states close to the Fermi energy are able to capture the shape of the Fermi surface.

2.6. Scaling and Related QMC Methods

The QMC computational demands as a function of problem size, type of atoms, number of electrons, and sampling techniques can be characterized in several ways. If we skip over details of implementations, hardware, parallelization, etc., the total computational time can be written as

$$T_{\text{tot}} \propto T_{\text{sam}} K_{\text{dec}} \frac{\sigma_E^2}{\epsilon^2} \quad (15)$$

where T_{sam} is the time needed to calculate the required quantities (wave function, energy, etc.) per one propagation step, σ_E^2 is the local energy variance (eq 8), K_{dec} is the number of propagation steps needed for a statistically independent sample, and ϵ is the target error bar. For large systems, the variance is proportional to the number of electrons $\sigma_E^2 = \sigma_0^2 N$, where σ_0^2 is the asymptotic value per single electron. Note that although the electrons are correlated, in large systems, the correlation and the contributions to the variance become statistically independent. The time to perform one propagation step with all coordinates updated is given by

$$T_{\text{sam}} \propto N^2 + c_3 N^3 \quad (16)$$

where the quadratic term includes evaluation of orbitals for the Slater matrix, pair Jastrow terms and interactions, while the cubic term corresponds to the calculation of determinants. Since $c_3 \ll 1$, typically 10^{-3} – 10^{-4} , up to about a thousand electrons, the quadratic term dominates, and therefore, the overall scaling is approximately $\approx N^3$ (see ref 89). This scaling can be improved to some extent by localizing the orbitals, by finite range Jastrow factors and possibly other trade-offs. Note that localization of orbitals and sparse matrix algorithms can make the impact of the determinant evaluations in very large systems less of an issue.^{150,151}

For practical calculations, it is important to have some idea how the overall time demands compare with commonly used mainstream methods such as DFT. Typically, the QMC calculations are slower by a factor of 10^2 – 10^5 when compared with DFT runs, depending on the system, type of Ψ_T , and required statistical accuracy (for instance, calculation with a target error bar of 0.1 kcal/mol is roughly a hundred times more

expensive than for statistical uncertainty of 1 kcal/mol). The price of the QMC accuracy is therefore significant, although availability of large parallel machines makes such calculations both feasible and practical. In addition, the statistical nature of QMC algorithms make them very suitable for large-scale parallelizations and indeed QMC belongs to the group of algorithms that harness the power of such machines very effectively.¹⁵²

The presented scaling applies only if we assume that with the increasing system size the decorrelation time remains constant. For the commonly used DMC algorithms, this is not strictly true, since the growth of σ_E^2 in large systems makes the DMC branching algorithm inefficient.¹⁵³ Depending on the types of atoms, this inefficiency comes to the forefront for sizes with more than 1000 valence electrons or so. More robust algorithms that can expand the applicability of the projector QMC methods beyond this limit require better sampling strategies and further development.

We note that for small systems, the massive-scale parallelizations are not really necessary (e.g., first two rows atoms are basically laptop problems, small molecules with 1 kcal/mol accuracy are workstation class problems, etc.). For larger systems or much higher accuracies, the massive parallelism is of significant importance but creates also some additional burden in implementation. Even seemingly simple tasks such as, for example, cloning the data for molecular/solid orbitals across a large parallel platform requires additional effort and expertise. Note that wave function files for large periodic supercells could be of significant sizes and might become the limiting factor of such calculations, especially if an accurate 3D spline representation is used. Another complication is the equilibration time and also possible need for a decorrelation period if all processors/cores start from the same set of configurations. Starting from scratch for each processor or core is, of course, possible; however, it would require that some time was discarded to allow for equilibration (several a.u. in the projection time, possibly more for wave functions with large areas of low densities and/or orbitals with long tails). In this discussion, we also assume that the parallelization is done along the walker axis, that is perhaps the easiest to implement. For very large system sizes, one might run into memory limits and parallelization along other domains (for example, orbitals) might be necessary. This is significantly more involved although still feasible. However, these are mostly technical problems that can be overcome with qualified effort and so far experience suggests that performance can be tuned up so that impressive calculations, like magnetic states in solids^{154–157} or large noncovalent systems,^{83,84,158–160} are feasible.

Perhaps the last point to mention here is the development of QMC methods that are based on other types of stochastic sampling such as auxiliary-field QMC,¹⁶² FCIQMC,¹⁶³ Hilbert-space Jastrow-coupled antisymmetric geminal power,^{164,165} or QMC with matrix product states¹⁶⁶ that are constructed around sampling the space of determinants rather than particle positions. These approaches have brought new insights and have produced very impressive results.^{167–169} Indeed, the development of stochastic methods is far from being exhausted and belongs to some of the most rapidly progressing areas in many-body quantum physics and chemistry.

2.7. Practical QMC Computations

Lest us sketch an example of a typical QMC calculation assuming a system with optimized geometry. The typical stages (Figure 5)

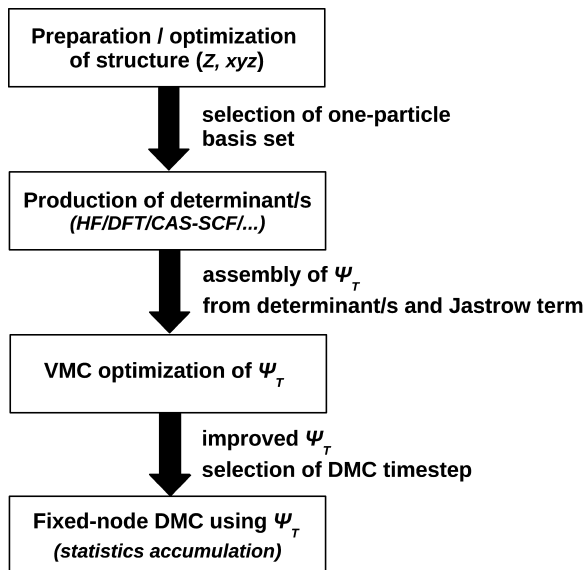


Figure 5. Sequence of stages that are involved in a typical QMC calculation.

include: (i) selection and construction of the antisymmetric part of Ψ_T ; for the Slater-Jastrow wave function the one-particle orbitals and coefficients of multideterminant expansions are precalculated within a self-consistent theory such as HF, DFT, CI, MCSCF, etc. It is, of course, crucial whether sufficiently accurate wave functions are available at the cost that is significantly smaller than is the total time required for the FNDMC. In this respect, the recent developments in methods such as CIPSI (configuration interaction using a perturbative selection of configurations in an iterative manner) advanced by Scemama and Caffarel look very promising.^{170–172} (ii) Variational improvement of Ψ_T from step (i) that may or may not improve the nodal surface, depending on the optimized parameter set. The optimized Jastrow factor does not affect the nodes and captures a significant fraction of electron correlations ($\approx 80\%$). (iii) FNDMC stage that uses the optimized Ψ_T as an input and includes equilibration and data collection periods.

Each of the stages (i–iii) involves a set of decisions to be made and also possible complications that may affect the final FNDMC results. More specific strategies strongly depend on the problem at hand. In section 3.3 below, we cover a number of technical details that affect the quality of FNDMC results for noncovalent interactions.

There are several computational packages that are available to carry out these tasks. Let us mention the codes QMCPACK¹⁷³ and QWalk,¹⁷⁴ as well as CASINO¹⁷⁵ and CHAMP.¹⁷⁶

3. NONCOVALENT INTERACTIONS BY QMC

As we outlined in the previous section, QMC has a number of important ingredients that make it attractive for a variety of many-body quantum problems, including challenges such as calculating very small interaction energies in noncovalent systems. We emphasize that the real-space FNDMC methods recover all possible many-body correlations within the nodal constraint $\Psi_T = 0$. This property makes QMC an interesting choice for noncovalent interactions in particular, since noncovalent interactions result from subtle long-range correlations that are spread across sizable parts of the configuration space. Fittingly, these are exactly the types of many-body effects where QMC is especially effective. Indeed, the demonstration that

QMC is able to produce results competitive with CCSD(T),^{66,67,78,84,137,177–179} and in some cases CCSDT(Q)⁵⁸ is already convincing for small systems, and similar performance is expected for larger systems. We will analyze this aspect further in the upcoming subsection on fixed-node error cancellation. Many unsolved questions, however, still remain open (see section 5).

Over the last three decades, QMC methods were applied to numerous applications that are directly or indirectly related to systems where accurate description of noncovalent interactions is crucial (see Table 1). These applications, extensively reviewed in the last section 4, include noble gases at ambient and extreme conditions, water clusters and ice phases, interactions of carbon-based and biomolecular materials with various molecular and atomic species, hydrogen storage systems, etc., some involving solid state systems with periodic boundary conditions or open-shell fragments.

In the following paragraphs, we continue with description of appropriate strategies useful for obtaining accurate FNDMC results.

3.1. Specific Considerations

For covalently bonded systems, the thermochemical accuracy of 1 kcal/mol is usually satisfactory^{117,180–183} and provides useful insights for processes such as bond formation/breaking in reactions and similar phenomena. However, benchmarks for noncovalent interactions require typically an order of magnitude higher accuracy, on par with the subchemical threshold value of 0.1 kcal/mol that poses a steep challenge for any computational method.

Note that technical parameters used in QMC calculations that make no or very little qualitative difference at the scale of 1 kcal/mol may play a decisive role in case of noncovalent interactions. The quality of QMC results depends considerably on parameters that enter the typical multistage computational sequence (Figure 5), since each step depends on its own set of technical parameters and/or user choices. One such set of parameters and choices includes selection, construction, and variational optimization of trial wave function ansatz. The FNDMC production step requires sufficiently long projection times that reach the desired states. Another relevant DMC aspect is checking the time step and population control biases. In addition, the biases coming from the treatment of ECPs must be kept under control as well. The related technical details are discussed in the following subsections.

3.2. Fixed-Node Bias Cancellation

As we briefly mentioned above, there have been a few recent studies of systematic effects that are at the origin of the fixed-node biases.^{120–122} It turned out that these errors, both in atoms and bonded systems, are influenced mainly by two key factors: electronic density and the node nonlinearity that is related to the bond length and multiplicity. In particular, an increase in the density typically leads to higher fixed-node biases. Similarly, in a bonded system, the fixed-node error grows with shorter bonds and higher bond multiplicities. These observations clarify why FNDMC hardly overcomes 1 kcal/mol accuracy in covalent bond breaking situations,¹¹⁷ and they also suggest that in some classes of systems, the fixed-node errors could be unexpectedly small. For example, for the Si crystal, one recovers more than 98% of the correlation energy for supercells with hundreds of electrons using just the nodes from a single-reference trial function. In the light of our arguments above, this is not too difficult to accept: Si in the diamond structure has only single

Table 1. List of References Where Noncovalent Interactions Were Studied by QMC (in Chronological Order) with Important Attributes Indicated (as Available in the Source)^a

year	first author	ref	system(s)	QMC method	Ψ_T	orbitals	Jastrow	ECP
1986	Ceperley	143	He dimer	GF-QMC, RN				
1990	Mohan	235	He trimer	FNDMC	HJ		2B	
1991	Caffarel	265	He dimer	PQMC				
1993	Anderson	236	He–He potential	EQMC				
1994	Bhattacharya	237	He ₃ symmetric	EQMC				
1994	Bhattacharya	237	H–He potential	EQMC				
1994	Pang	230	ionic H clusters	FNDMC	SJ		2B	
1996	Huiszoon	240	He–He	PQMC				
2001	Anderson	238	He–He potential	EQMC				
2001	Bokes	231	ionic H clusters	FNDMC				
2002	Filippi	260	H ₂ on Si(001)	FNDMC	SJ	(MC) HF		
2003	Mella	80	He ₂ , LiH	FNDMC	SJ	RHF		
2004	Anderson	239	He ₂ potential	EQMC				
2005	Diedrich	81	water, ammonia, and benzene dimer	FNDMC	SJ			
2005	Grossman	246	water	FNDMC + MD	SJ	PBE		
2006	Benedek	184	water dimer	FNDMC	SJ	HF, B3LYP	3B	loc
2006	Cicero	252	CNT w/small groups	FNDMC	SJ	DFT		
2006	Drummond	219	Ne solid	FNDMC	SJ	LDA	3B	loc
2006	Grimme	196	anthracene dimerization	FNDMC	SJ	B3LYP		
2006	Kim	197	H ₂ on B/Be-doped fullerenes	FNDMC	SJ	LDA		
2007	Drummond	259	vdW in metallic wires/layers	FNDMC	SJ-BF		2B	
2007	Gurtubay	137	water dimer	FNDMC	SJ	B3LYP	3B	
2007	Sorella	248	benzene dimer	LR-DMC	JAGP		3B	
2008	Attaccalite	225	liquid hydrogen at high pressure	VMC/DMC				
2008	Beaudet	204	benzene–H ₂	FNDMC	SJ, JAGP		3B+	loc
2008	Korth	82	adenine/thymine, cytosine/guanine, S22	FNDMC	SJ	HF	3B	
2008	Lawson	187	carbon nanotube–NO ₂	FNDMC	SJ	B3LYP	3B	loc
2008	Springall	194	He–He potential	FNDMC	SJ	HF	3B	
2008	Sterpone	241	water dimer	LR-DMC	JAGP		3B	
2008	Zaccheddu	199	triazine + NO ₃ ⁻	FNDMC	SJ	B3LYP	3B	loc
2008	Santra	177	water hexamer	FNDMC	SJ	B3LYP	2B	loc
2009	Kanai	250	benzene–small molecules	FNDMC	SJ	LDA, PBE	2B	
2009	Ma	178	benzene–water	FNDMC	SJ	LDA	3B	loc
2009	Spanu	251	graphite	LR-DMC	SJ	LDA	2B	
2009	Wu	200	MgH ₂	FNDMC	SJ	PBE		
2010	Bajdich	188	Ca ⁺ w/H ₂ and (H ₂) ₄	FNDMC	SJ, MDSJ	DFT/CAS-SCF	2B	loc
2010	Caffarel	254	thiophene–Li	FNDMC	SJ		3B	
2010	Hongo	261	para-diiodobenzene crystal	FNDMC	SJ	PW91	2B	
2010	Wu	195	He dimer potential	FNDMC, RMC	SJ	HF	3B	
2010	Morales	226	hydrogen under extreme conditions	FN-RMC				
2011	Korth	179	Thiophene–Li	FNDMC	SJ	PBE, B3LYP	2B	loc
2011	Ma	211	H on benzene, coronene, and graphene	FNDMC	SJ	LDA	3B	tm
2011	Ma	211	water on graphene	FNDMC	SJ			
2011	Raza	221	ice XI	FNDMC	SJ	LDA		loc
2011	Santra	220	ice	FNDMC	SJ	LDA		loc/tm
2012	Gillan	78	water clusters ($n \leq 6$)	FNDMC	SJ	LDA	3B	loc
2012	Horvathova	255	benzene–V	FNDMC	SJ	DFT	3B	loc
2012	Horvathova	255	benzene–V, –Co	FNDMC	SJ	DFT	3B	loc
2012	Hsing	217	O, F, H on graphene	FNDMC	SJ	LDA, PBE	3B	tm
2012	Jiang	218	H ₂ on C ₄ H ₃ Li	FNDMC	SJ	B3LYP		loc
2012	Karalti	212	water on MgO(100)	FNDMC	SJ	LDA	3B	loc
2012	Tkatchenko	158	C ₆₀ @C ₆₀ H ₂₈ , GLH@mcycle	FNDMC	SJ	LDA	3B	loc
2013	Xu	206	water dimer, benzene–water	FNDMC	SJ	LDA, HF	3B	tm, loc
2013	Alfe	242	water droplets/bulk	FNDMC	SJ	LDA	3B	loc
2013	Gillan	222	water clusters/ice	FNDMC	SJ	LDA		loc
2013	Hongo	191	A/T step in B-DNA	FNDMC	SJ	SVWN, PBE, B3LYP	3B	tm
2013	Dubecky	66	subset of S22, HF dimer	FNDMC	SJ	HF, B3LYP	3B, 3B distinct	tm
2013	Wang	210	(H ₂ O) ₁₆	FNDMC	SJ	B3LYP	3B	tm
2013	Granatier	257	benzene–Pt	FNDMC	SJ	TPSSH, M11	2B	loc
2013	Shulenburger	149	soild Ar, Kr, and Xe	FNDMC	SJ	LDA	2B	tm

Table 1. continued

year	first author	ref	system(s)	QMC method	Ψ_T	orbitals	Jastrow	ECP
2014	Alfe	243	compressed water	FNDMC	SJ	LDA		loc
2014	Ambrosetti	83	large host–guest complexes	FNDMC	SJ	LDA	3B	tm
2014	Benali	84	noble gases, DNA-clipcine	FNDMC	SJ	LDA	2B	loc
2014	Chen	215	hydrogen under pressure	FNDMC	SJ	LDA	2B, 3B	loc/tm
2014	Cox	201	sI methane hydrate	FNDMC	SJ	PBE	3B	
2014	Deible	202	CH_4 in $(\text{H}_2\text{O})_{20}$	FNDMC	SJ	B3LYP	3B	tm
2014	Dubecky	79	subset of S22, A24	FNDMC	SJ	B3LYP	2B	tm
2014	Ganesh	214	Li–graphite	FNDMC	SJ	PBE	2B	loc
2014	Al-Hamdani	67	BN-doped benzene–water	FNDMC	SJ	LDA, PBE	3B	loc
2014	Mazzola	227	hydrogen under pressure	VMC				
2014	Morales	244	bulk water	FNDMC	SJ	PBE	3B	tm
2014	Quigley	245	ice	FNDMC	SJ	LDA		loc
2014	Misquitta	272	three 1D wires	FNDMC	SJ		2B	
2014	Shulenburger	192	Xe solid	FNDMC	SJ	LDA, AM05		
2014	Drummond	185	molecular hydrogen at extreme pressures	FNDMC	SJ	PBE	3B	
2015	Gillan	68	CH_4 –water	FNDMC	SJ	LDA		loc
2015	Al-Hamdani	160	h-BN–water	FNDMC	SJ	LDA	3B	loc
2015	Wu	161	h-BN–water	FNDMC	SJ	PBE	2B	
2015	Hongo	193	para-diiodobenzene crystal	FNDMC	SJ	LDA, GGA, B3LYP	2B	tm
2015	Kocman	232	coronene– H_2	FNDMC	SJ	B3LYP	2B	tm
2015	McMinis	228	hydrogen phase transition	FNDMC	SJ	PBE	2B	
2015	Rezac	58	dimers of H_2O , HF, CH_4 , NH_3	FNDMC	SJ	B3LYP	3B, 3B pol	tm
2015	Zen	267	water	VMC				
2015	Tubman	229	hydrogen under pressure	FN-CEIMC		DFT		
2015	Deible	190	Be_2	FNDMC	SJ, MDSJ	HF/DFT/CAS	3B	loc
2015	Azadi	249	benzene dimer	FNDMC	SJ, SJ-BF	LDA	3B	tm
2015	Mostaani	159	bilayer graphene	FNDMC	SJ	LDA	2B	loc
2016	Amovili	253	CH_4 dimer	FNDMC	SJ	PBE0	3B	tm
2016	Clay	234	H/He mixtures	FNRMC	SJ	PBE	2B	

^aAbbreviations: GF, Green's function; RN, released node; PQMC, perturbative QMC; EQMC, exact QMC; RMC, reptation MC; LR, lattice regularized; MD, molecular dynamics; CEIMC, coupled electron ion Monte Carlo; HJ, Hylleraas-Jastrow; SJ, Slater-Jastrow; BF, backflow; MDSJ, multi-determinant SJ; JAGP, Jastrow-antisymmetrized geminal power; 2B, Jastrow factor with up to 2-body terms; 3B, Jastrow factor with up to 3-body terms; loc, locality approximation; tm, Casula T-moves.

bonds that are longer than, say, in carbon systems, and the valence electron density is moderate.¹²²

For our purposes, it is important that most of the noncovalent interactions can be characterized by low densities in the dispersive bonding region, large bond lengths with σ -like character, and mostly single-reference nature of the wave functions. Clearly, all of these play into the strengths of the QMC method. The key challenge is how to maintain the high systematic accuracy for the noncovalent complex consisting of monomers that nominally contain covalent bonds and therefore carry along some associated fixed-node biases.

One possibility is to rely on the error cancellation by keeping the constructions and optimizations of the corresponding wave functions as systematic as possible. This has turned out to be very important due to the fact that it enables us to cancel out the monomer fixed-node errors in total energy differences almost exactly. The conceptual explanation of this fact is given in Figure 6. Note that the superimposed dimer and monomer nodes are almost identical in the monomer region (Figure 7). One can expect that the nodal errors in the monomer regions will be very similar and therefore will largely cancel out. On the other hand, the dispersive interaction is located in the low-density region where contributions from the exchange are negligible and, consequently, the impact of nodal errors is strongly diminished. We note that this finding has been extensively discussed^{66,80} and observed in a number of QMC studies of closed-shell systems (refs 58, 66, 67, 79, 81, 82, 84, 177–179, and 184).

This cancellation therefore relies on keeping the nodes at the same systematic accuracy at every step of the trial wave functions constructions. In particular, the same self-consistent method is used to generate the orbitals, and the antisymmetric part of the wave functions should have the same form (e.g., single reference).

It is perhaps somewhat counterintuitive, that effort to improve the nodes by including node optimizations in the trial function construction in this context might be less effective or simply impractical. The demands on keeping the systematic accuracy (e.g., in optimization of the nodes in monomers as well as in the noncovalent complex might be so high that the statistical noise could overshadow the important energy difference signal). Note that optimizations of nodes¹⁸⁵ require very large walker populations and often many more iterations than with the nodes kept intact. In some cases, it has been observed that somewhat less accurate but systematically consistent trial wave functions have provided more accurate results, for instance, in calculations of water dimer with the single-reference Slater-Jastrow versus the same boosted with the backflow coordinates.¹³⁷

In cases where the fixed-node error cancellation provides desired accuracy, it has proved to be a very effective strategy. The available results (Table 1) are very promising and indicate a domain of reliable and practical calculations such as closed-shell *s/p* complexes at equilibrium.⁹⁹ More research is clearly needed

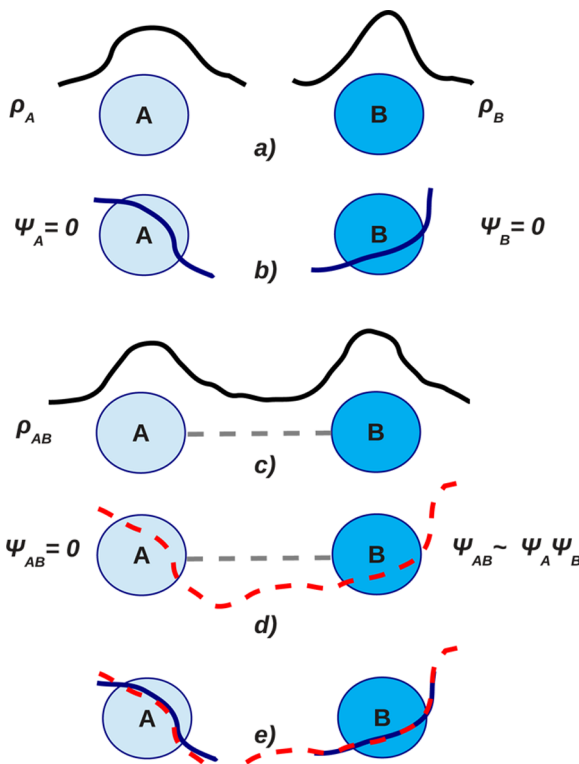


Figure 6. Qualitative sketch of the origin of fixed-node error cancellation in van der Waals complexes. (a) The isolated monomer molecules A and B described by the approximate wave functions Ψ_A and Ψ_B , related one-electron densities ρ_A and ρ_B , and (b) the corresponding nodal surfaces, $\Psi_A = 0$ and $\Psi_B = 0$; (c) weakly interacting closed-shell system $A + B$ with the approximate wave function Ψ_{AB} and ρ_{AB} ; (d) the nodal surface $\Psi_{AB} = 0$; and (e) superimposed nodal surfaces of the dimer and the monomers. Note that the nodal surface of the dimer closely follows the nodal surfaces of monomers in the regions of large exchange effects and high densities. Since the overlap of Ψ_A and Ψ_B is small, the exchange effects in the bonding region are negligible. Significant fixed-node error cancellation is therefore expected in FNDMC energy differences, assuming that the same systematic construction was used for Ψ_A , Ψ_B , and Ψ_{AB} . This effect has been visually analyzed and confirmed,⁶⁶ see also ref 99.

in this direction, for example, some discrepancies were detected in dimers of HCN and formaldehyde.⁷⁹

3.3. Practical Aspects

The main source of FNDMC errors is the approximate Ψ_T which determines the fixed-node bias and in the presence of ECPs, also bias from the localization approximation. Besides that, further sources of possible errors exist: population control bias, DMC time step bias, or treatment of noninteracting monomers reference energy (it matters whether one obtains the total energies of monomers separately or in a single run with monomers separated reasonably far from each other²⁰⁶). As we indicated, the calculations should be organized in such a manner that the composite system and the monomers are described on the same footing, and in addition, it is necessary to check that the technical errors are under control while the cancellation in energy differences is maximized.

3.3.1. Trial Wave Functions. Although several types of many-body wave function ansatze have been developed and applied in QMC (section 2.2), for noncovalent interactions, the single-reference Slater-Jastrow wave functions currently dominate (see Table 1). This has resulted both from simplicity and

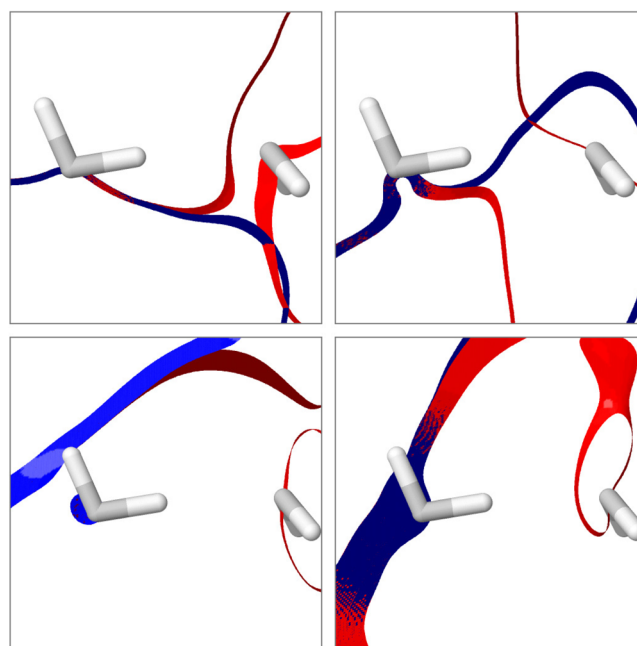


Figure 7. Illustration of the nodal surfaces for the water dimer (red)⁹⁹ and the left water monomer (blue).⁹⁹ Depicted are subsets of the nodal surfaces obtained by scanning the space by one electron, while the rest of the electrons are kept fixed at snapshot positions. For better visibility, only slices of the surfaces that lie between two parallel planes are visualized. Note that in the region of the monomers, the nodal surfaces lie on top of each other. For the conceptual explanation, see Figure 6.

from satisfactory results that were obtained in most cases. It is also clear that parametrizations of Ψ_T , which involves one-particle orbitals, basis sets, and Jastrow parameters, affect the quality of the production results. Multireference Slater-Jastrow wave functions¹⁸⁶ were applied only in a limited number of cases.^{187–190} One can expect wider use of multireference wave functions in the future, in particular for complexes with more pronounced multireference character or in studies of open-shell complexes.

3.3.2. One-Particle Orbitals. The orbital choices in Slater-Jastrow FNDMC calculations have been studied quite extensively.^{66,79,178,179,184,191–193}

Benedek et al.¹⁸⁴ performed all-electron FNDMC calculations, in water dimer, with Slater-Jastrow wave functions using HF and B3LYP orbitals. The results were found to be compatible with CCSD(T) and indistinguishable within 1σ error margin (HF: 5.02 ± 0.18 kcal/mol, B3LYP: 5.21 ± 0.18 kcal/mol).

In the water–benzene complex, Ma et al.¹⁷⁸ compared trial wave functions constructed with one-particle orbitals from LDA, PBE, PBE0, B3LYP, and HF in three representative molecular configurations. The FNDMC energy differences with DFT orbitals were compatible within a statistical uncertainty of $\approx 3\sigma$, and the best agreement with CCSD(T) calculations was found for the LDA orbitals, while the HF orbitals produced the trial wave function with slightly higher total energies.

In 2011, Korth et al. showed that in ECP-based FNDMC calculations of Li–thiophene complex,¹⁷⁹ one-particle orbitals from B3LYP and PBE with the VTZ basis set produced essentially identical interaction energies, namely -8.2 ± 0.1 and -8.3 ± 0.1 kcal/mol, respectively, whereas HF orbitals produced an interaction energy of -7.0 ± 0.1 kcal/mol. The observed difference between DFT- and HF-based trial functions possibly

indicates less accurate fixed-node bias cancellation in charge-transfer complexes.

Hongo et al. reported FNDMC stacking energies of the B-DNA step, using HF, LDA, GGA, and hybrid B3LYP DFT orbitals in Ψ_T . The results were found to be compatible within the statistical uncertainty and also with the CCSD(T) reference.¹⁹¹

In multiple weakly bounded small complexes, Dubecký et al. observed that B3LYP and HF orbitals used in Slater-Jastrow trial wave functions produce essentially identical FNDMC interaction energies, within the statistical uncertainty converged to approximately ± 0.07 kcal/mol.^{66,79}

Hongo et al. studied noncovalent crystal polymorphism of para-diiodobenzene by FNDMC.¹⁹³ For three types of DFT orbitals calculated within LDA, PBE, and B3LYP, with the Ewald treatment of Coulomb interactions in periodic supercells ($1 \times 1 \times 1$, $1 \times 3 \times 3$ only by PBE) and T-moves method for ECPs, all three functionals produced results compatible within the statistical error. With the model periodic Coulomb interaction, the FNDMC results varied more significantly and differed also qualitatively: it was observed that the phase stability changes depending on the functional used to generate the orbitals. Clearly more research is needed for periodic systems that are further complicated by the finite size extrapolations.

Although very reasonable interaction energies were obtained with one-particle orbitals from HF,^{66,79,82,184,194,195} orbitals from the Kohn–Sham self-consistent calculations are often preferred (e.g., refs 78, 177, 179, 187, 192, and 196–202), since they typically lead to lower total FNDMC energies^{66,178,191} and properties more consistent with experiment and/or benchmarks.^{136,179,186,203}

3.3.3. Basis Sets. In general, one-particle orbitals are expanded in continuous basis functions or evaluated on a real-space grid. Due to their analytical properties, plane waves and Gaussians (or Slater orbitals expanded in Gaussians) are frequently chosen as primitives in self-consistent methods as well as in QMC. Gaussians are convenient to use also due to the availability of extensive and systematically developed basis sets; nevertheless, for noncovalent interactions additional care should be taken when choosing the appropriate basis. The most important deficiencies are similar as for the self-consistent methods such as incompleteness and/or saturation of the basis, basis set superposition errors, and linear dependency problems if they are locally too numerous and/or generally too diffuse. Unphysical quadratic exponential decay of Gaussian tails may cause sampling errors as well.^{81,204}

In a familiar example of the 1s orbital in a hydrogen-like atom, Diedrich et al.⁸¹ have illustrated that for any finite Gaussian expansion, there exists a radius where quantum force and local energy start to diverge (see Figure 8). Therefore, it pays off to improve the orbitals in the tail regions,²⁰⁵ for example, by including smaller exponent(s) into the Gaussian-expanded contractions, by using numerical approximation for the radial part of the orbital or by including functions with right asymptotic behavior (Slater-type orbitals). It also pays off to improve orbitals around nuclei (e.g., by including larger exponents into contractions²⁰⁶ or by adding exact cusp into the Jastrow factor). The resulting decrease of the fluctuations can be significant and improves the robustness of the calculations.

Diedrich et al.⁸¹ also noted that large Gaussian basis sets improve asymptotic description of tails significantly but may lead to linear dependency problems. It was found that HF trial wave functions built upon aug-QZV bases led to reasonable FNDMC

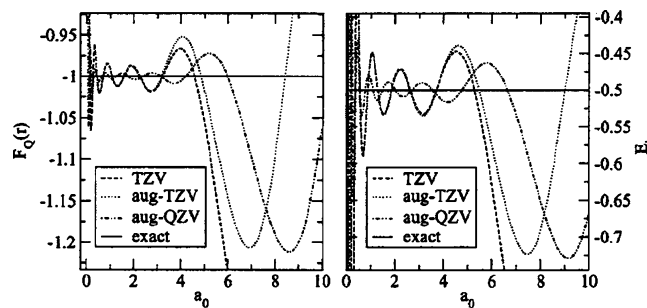


Figure 8. Drift (left panel) and local energy (right panel) for the hydrogen 1s orbital expanded in various Gaussian basis sets. The total energies are -0.4998098 au(TZV), -0.499821 (aug-TZV), and -0.499984 au (aug-QZV).⁸¹ Reprinted with permission from ref 81. Copyright 2005 AIP Publishing LLC.

results for the methane dimer but not for benzene dimer in the parallel displaced geometry. This was attributed to a poor description of the nodal surface in the dimer case due to the orthonormalization of large, almost linearly dependent basis set. The FNDMC with the Slater determinant constructed from nonorthogonal monomer orbitals yielded a significantly better result in this case.

We also note that spurious nodes (that generate artificial nodal pockets) were detected^{207,208} due to incompleteness of the Gaussian basis sets; nevertheless, its effect on FNDMC energies was not clearly visible.²⁰⁸ Most probably, the contributing overall weight of such artificial features was low as the DMC walkers in the isolated high-energy regions simply die out in the long projection time limit.

Beaudet et al. studied the benzene–H₂ complex using the VTZ basis set augmented with diffuse functions from aug-cc-pVTZ basis with PBE orbitals and two-body Jastrow. This simple wave function produced energy-distance curves compatible with FNDMC based on fully optimized Jastrow correlated single determinant geminal wave functions, signaling thus high degree of the fixed-node bias cancellation when using simple Slater-Jastrow ansatz.²⁰⁴

Korth et al. reported on the difference between noncovalent interaction energies of the Li–thiophene complex obtained with VTZ (-8.2 ± 0.1 kcal/mol) and VQZ (-8.7 ± 0.1 kcal/mol) basis sets (PBE). The results from VQZ basis were close to the CCSD(T)/CBS reference of -8.8 ± 0.1 kcal/mol.¹⁷⁹

Additional tests of basis set cardinality (i.e., VnZ with increasing n)²⁰⁹ between VTZ and VQZ versus the effect of added augmentation functions has been studied by Dubecký et al. in ammonia dimer⁶⁶ with B3LYP orbitals. It turned out that while the higher cardinality lowers the local energy variance and therefore the statistical convergence rate is somewhat faster, it has a smaller effect on the overall accuracy than the augmentation functions. In fact, the additional diffuse functions were found to be crucial to reach the reference CCSD(T)/CBS interaction energy value (-3.15 kcal/mol).⁵⁶ In particular, the VTZ and VQZ bases generated values of -3.33 ± 0.07 and -3.47 ± 0.07 kcal/mol, respectively, that were less accurate. The augmented bases (aug-VTZ and aug-VQZ) produced energy differences of -3.10 ± 0.06 and -3.13 ± 0.07 kcal/mol, respectively, and the aug-VTZ basis set was recommended as the most reasonable choice with respect to price/performance ratio. As mentioned above, the likely effect of augmentation functions are improved tails that are crucial for van der Waals complexes.

Xu et al.²⁰⁶ observed that saturated contractions of occupied shells reduce time step errors and improve convergence of FNDMC calculations when compared with contractions with smaller number of primitives.

Another basis set modifications that appear in the QMC literature dealing with noncovalent interactions include judicious trimming of the basis, addition of augmentation functions and their reoptimization, or (manual) adjustment. We note that system specific reoptimizations or adjustments are not recommended because the favorable FN-error cancellation may be diminished.

Trimming of high-angular momentum basis functions is motivated by the fact that the recovery of correlation in FNDMC happens in a very different manner than in basis set correlated wave function methods. For example, Springall et al. observed negligible influence of *d* and *f* Gaussian basis functions on the interaction energy of He dimer.¹⁹⁴

As we mentioned above, the addition of limited number of augmentation functions sometimes leads to improved stability of calculations and makes sampling in the tail regions more efficient. Zucchetti et al. used extensive augmentation in calculations of triazine and NO_3^- in distant configuration.¹⁹⁹

Optimization of augmentation functions enables sampling error reduction with lower number of basis functions. For example, MP2-optimized augmentation functions were employed by Mella and Anderson.⁸⁰

Wang et al. studied large water cluster²¹⁰ using combination of atomic *sp* functions from the aug-cc-pV5Z-CDF²⁰⁶ basis set, further augmented by *d* functions on oxygen and *p* functions of hydrogen. Note that some of the exponents had to be adjusted in order to avoid linear dependency problems.

3.3.4. Explicit Correlation. While in the fixed-node cancellation scheme, the determinantal part remains fixed, the Jastrow term is always optimized in order to lower the variance of local energy that reduces CPU cost of DMC calculations. In addition, in the presence of ECP, the improvement of the trial wave function is important for lowering the systematic bias from approximate treatment of ECP. The following questions are therefore vital: how the quality (complexity) of the Jastrow factor affects the quality of the FNDMC energy differences in weakly bonded complexes? In other words, apart from the fixed-node bias, how the errors coming primarily from the localization approximation of ECP cancel out? What is the desired complexity of the Jastrow term to reach a reasonable cost/accuracy trade-off?

Although the isotropic three-body Jastrows containing up to electron–electron–nucleus correlations are frequently used,^{78,185,211–213} much less costly⁷⁹ two-body isotropic Jastrows were found to be reliable enough in numerous cases (e.g., refs 84, 179, and 214). It has been observed that optimized three-body versus two-body Jastrow factors lower the variance and improve quality of FNDMC results only slightly.^{79,215} Experience shows that three-body Jastrows¹⁹³ also slightly improve description of stacking and interactions of atoms with molecules.⁷⁹ However, on average for larger molecular sets, the results from three-body and two-body correlation schemes appear to be similar.⁹⁹

The Jastrow terms are most often used in a setting with one parameter set per atomic species. An additional variational freedom comes with the distinction of all atoms or atom types. For example, isolated water dimer contains two types of oxygens, that may be treated separately, and two types of hydrogen (the one that contributes to the hydrogen bond and those away from the hydrogen bond region). The contribution from the three-

body Jastrow with distinct atom types has led to a slightly improved FNDMC interaction energy of water dimer by about 0.1 kcal/mol.⁶⁶

Finally, one can exploit anisotropy and add polarization terms to the Jastrow helping thus to achieve more variational freedom.⁵⁸ These fine improvements are adding small fractions of kcal/mol to the interaction energies and enable systematic improvements. However, so far their cost prevents routine use.

3.3.5. Variational Cost Function. Variational improvement of the Jastrow terms is crucial for reducing the local energy fluctuations so that the costly FNDMC calculations can be less extensive. In the presence of ECPs, however, the FNDMC results are not solely dependent on the nodes of Ψ_T but also on an additional nonlocal ECP term (eq 10). The corresponding localization approximation requires the trial wave functions to be accurate not only in the location of nodes but also in the region of the ECP nonlocality (section 2.4).

The variational improvement of trial functions used in DMC may be accomplished with the help of several cost functions [e.g., based on variance, energy, or their linear combinations (section 2.3)]. Even though the variance optimization is widely used, the minimization of energy was found to provide systematically better related expectation values.^{129,216} For example, it was observed that the variance and energy-optimized three-body Jastrow factors lead to different FNDMC results in the ammonia dimer.⁷⁹ While the energy-optimized (95% of energy and 5% of variance) trial wave function in FNDMC led to the interaction energy of -3.10 ± 0.06 kcal/mol, that is consistent with the reference CCSD(T)/CBS value of -3.16 kcal/mol,⁵⁶ the variance-optimized result of -3.28 ± 0.04 kcal/mol deviated by more than 3σ from the reference. On the other hand, many other results in noncovalent systems confirm that variance optimized trial wave functions suffice (e.g., refs 78, 159, 177–179, 202, 210, 215, 217, and 218), presumably still due to the bias cancellations in weakly bound complexes. The problem of selection of VMC cost functions in this application area is therefore not fully settled yet.

3.3.6. Diffusion Monte Carlo. With the assumption that the optimization of trial function has been carried out, one proceeds to FNDMC production runs. Each FNDMC calculation consists of equilibration and statistics accumulation periods. The technical settings of FNDMC total energy calculations that affect results include the DMC time step setting, walker population size, and effects of possible approximations used for the treatment of ECPs.

Mella and Anderson found no DMC time-step dependence of the interaction energy in He_2 at equilibrium for four values of time steps between $\tau = 0.007$ and 0.0015 au.⁸⁰

In all-electron FNDMC calculations of water dimer with HF nodes, Benedek et al. observed that for small time steps less than or equal to 0.005 au, the interaction energies were converged to the value statistically consistent with the time step extrapolation.¹⁸⁴

Drummond and Needs, in their study of solid neon,²¹⁹ observed steady decrease of the total energy with the decreasing time step in the range of 0.03 – 0.002 au. On the other hand, they found that the static lattice pressure of the studied solid is insensitive to the time step and identical results were obtained with time steps of 0.001 and 0.0025 au.

Grimme et al. in their study of anthracene dimerization¹⁹⁶ checked the time step dependence of the FNDMC results by performing tests with 0.005 and 0.003 au and found that the

energy differences were compatible within the target accuracy of 1 kcal/mol.

Gurtubay and Needs extensively tested the time step dependence of the total FNDMC energies and interaction energies in water dimer, in calculations using all-electron and ECP schemes, both when using the localization approximation and as well as T-moves.¹³⁷ Notably, in calculations with ECPs, the localization approximation and T-moves led to different total energies (in dimer by about 4 mHa) at the zero time step limit. However, a high degree of the time step error cancellation was observed in the final interaction energies from both ECP treatments (Figure 9), giving very similar results, -5.03 ± 0.07 and -5.07 ± 0.07 kcal/mol, respectively.

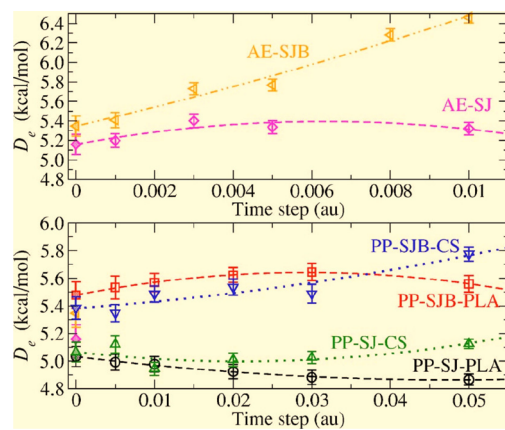


Figure 9. Dependence of FNDMC all-electron (top panel) and ECP-based (bottom panel) dissociation energies of the water dimer on the time step and treatment of ECP. Abbreviations: AE, all-electron; PP, pseudopotential (ECP); SJ, Slater-Jastrow; SJB, SJ-Backflow; CS, Casula T-moves; and PLA, localization approximation. Reprinted with permission from ref 137. Copyright 2007 AIP Publishing LLC.

Lawson et al. assessed time step errors of the production FNDMC runs using 0.1 au time step, by additional calculations using the time step of 0.05 au. The changes of the energy differences amounted to ~ 1 kcal/mol, that was of the order of the desired statistical uncertainty.¹⁸⁷

Ma et al. studied the benzene–water interaction¹⁷⁸ and interaction of hydrogen with benzene coronene and graphene.²¹¹ For binding energies, no differences within 5 meV were observed between FNDMC runs with 0.0125 and 0.005 au time steps.

Localization approximation and T-moves schemes were tested in calculations with ice supercells by Santra et al.²²⁰ using the time steps between 0.001 and 0.005 au. The T-moves FNDMC energies showed steep linear trend and allowed convenient zero time step extrapolation, while the localization approximation showed nonlinear but a more flat trend. It was found that both schemes provide statistically compatible energy differences, which indicates ECP-bias error cancellation. Due to its more moderate time step dependence, the localization approximation was used for the production runs with a time step of 0.002 au.

The cohesive energies of ice in large supercells from FNDMC were found to be converged within 5 meV per the water molecule, with the localization approximation and time step of 0.002 au.²²¹

In the study of small water clusters by Gillan et al., the time step of 0.005 au was found to provide total energies converged to 0.4 mHa.⁷⁸ In the subsequent study of water and ice, the time step of 0.002 au within the localization approximation was used

and checked against the run with the time step of 0.0005 au. No change in the total energy was found within the error of 0.5 mHa.²²² Similarly, in the water–methane system, the time step of 0.005 au was used and checked against 0.002 au, showing acceptable differences, smaller than 0.3 mHa/monomer.⁶⁸

Tkatchenko et al. found that the time step of 0.005 au used with the localization approximation in FNDMC suffices to treat large host–guest complexes. The tests included time steps of 0.0125, 0.005, and 0.002 au.¹⁵⁸

Xu et al. studied the time step bias dependence on the basis sets and reference level calculation strategies. They observed significantly reduced time step dependence of FNDMC water binding energies when the reference energy level was calculated using both monomers in distant configuration instead of calculations with separate monomers.²⁰⁶

In larger systems including water clusters²¹⁰ or molecules in large cages,²⁰² the time step bias of the noncovalent FNDMC interaction energies was significant in some cases and testing of the time step bias and/or extrapolations were strongly recommended.

Ambrosetti et al. tested robustness of interaction energies versus ECP treatment approximation and time step⁸³ in a large host–guest complex. For comparison, with LDA orbitals, and time step of 0.005, the T-moves and localization approximation resulted in the interaction energies of -26.5 ± 1.2 and -27.4 ± 1.2 kcal/mol, respectively, while with $\tau = 0.001$ au and T-moves, the interaction energy was -26.7 ± 1.2 kcal/mol. The T-moves scheme and a time step of 0.002 au were selected for the production calculations.

In study of Li-intercalated graphite, Ganesh et al. used FNDMC time step of 0.02 au. The test in bulk graphite with $\tau = 0.005$ au has shown that the total energy converges to 10 meV per carbon atom.²¹⁴

Al-Hamdan et al., in the study of hexagonal boron nitride surface interacting with water used a time step of 0.015 au that provides converged results versus a time step of 0.005 au.¹⁶⁰

Hongo et al.¹⁹³ observed that the T-move scheme improves numerical stability as it helps to avoid walker population explosion problems and allows use of larger time steps.

3.3.7. Summary. At the current stage of development, the FNDMC protocol with maximized error cancellation can be outlined as follows. It provides very favorable trade-off in the price/performance ratio for calculations of closed-shell noncovalent interactions in *s/p* complexes. (i) Reference energy: estimation of the noninteracting reference energy should be done with sufficiently separated monomers in a single calculation. (ii) Ψ_T : Slater-Jastrow type wave functions with B3LYP orbitals expanded in an augmented valence triple- ζ or better basis (alternatively, in plane waves basis with very high-energy cutoff) and Jastrow factor containing at least electron–electron and electron–nucleus terms. (iii) VMC: exhaustive optimizations based on robust algorithms that are driven by energy minimization should be employed. (iv) DMC: ECPs should be treated beyond locality approximation (T-moves) with dense ECP integration grids, and a time step of 0.005 au or shorter should be used so that the time step errors are marginal and do not require extrapolations.

4. APPLICATIONS

In this section, the published QMC papers dealing with noncovalent interaction energies are reviewed (Table 1) and sorted according to criteria relevant for application areas such as materials science, chemistry, and physics. This provides a fast

lookup reference for the readers interested in specific topics and/or classes of materials and compounds. Each reported work is described only from the QMC perspective (i.e., other methodologies mentioned in the considered papers are mostly not commented upon). Properties and insights other than energy differences are included in the last subsection 4.11.

There are few applications that are somewhat at the borderline (i.e., topics that require exceedingly accurate description of intermolecular noncovalent interactions but do not belong to the general area of noncovalent interactions and are not listed below). The reader is referred directly to the original publications. These studies include study of interactions in hemibonded radical cationic dimers of He, NH₃, H₂O, HF, and Ne¹⁹⁸ and binding of excess electrons to water clusters.²²³

4.1. Hydrogen and Hydrogen Storage

Hydrogen is the most abundant element in the universe. Understanding of its phase diagram is not complete, and it still poses a significant challenge for both theory and experiment alike. The theoretical treatment of hydrogen at extreme conditions is involved, since it requires high quality and equal footing description of atomic and molecular phases (i.e., balanced description of intra- and intermolecular forces). QMC calculations provide here quite a unique set of results due to their accuracy, proper description of many-body effects, and explicit inclusion of periodicity.^{185,215,224–229}

Molecular hydrogen complexes represent the simplest clusters that can be studied by theory as well as by experiment. Ionic hydrogen clusters were studied by QMC methods in order to provide insights to electron correlation effects and possible structural motifs.^{230,231}

An important field is the problem of the hydrogen storage (i.e., storage of molecular hydrogen as a potential source of clean energy and related applications). The key task is to find materials with intermediate strength of H₂ binding that could potentially serve as hydrogen storage substrates. Binding of H₂ is in general very weak and requires balanced description of weak charge transfer and van der Waals effects that is challenging from a theoretical point of view. Benchmarks are required to assess cheaper methods (e.g., DFT) useful for screening of large complexes. QMC serves here as one of the viable choices.

Adsorption of H₂ in fullerenes doped by light-elements (B, Be) was studied by Kim et al.¹⁹⁷ Light-metal hydrides are among the promising materials for reversible storage of hydrogen. Wu et al. applied FNDMC to study desorption energy of H₂ from MgH₂.²⁰⁰ Bajdich et al. studied cationic clusters of Ca⁺ with single and four attached H₂ molecules using FNDMC.¹⁸⁸ Jiang et al. reported on a FNDMC study of H₂ attachment on C₄H₃Li molecule.²¹⁸ Adsorption of H₂ on coronene was studied by FNDMC in the work of Kocman et al.²³²

Finally, we include the studies where interactions of atomic hydrogen with various substrates were considered: accurate H–He potential was obtained by Bhattacharya and Anderson using the exact reformulation of the QMC method.²³³ The interactions of atomic H with benzene, coronene, and graphene were studied by Ma et al.²¹¹

Clay et al. benchmarked various DFT functionals versus QMC in H/He mixtures including high-density configurations.²³⁴

4.2. Noble Gases

In the early days of QMC, theoretical treatment of noble gases, especially He quantum liquids, were of high importance in low-temperature physics. QMC approaches were among the first to provide benchmark numbers, and noble gases became important

applications for testing accuracy of new methodologies including FNDMC.

The He–He potential was studied by Ceperley¹⁴³ using Green's function QMC and released-node methods, and by Anderson^{233,235–239} using exact QMC method applicable to very small systems. Later on, FNDMC was found to provide reliable results in this prototypical system.^{80,194,195} Perturbation QMC²⁴⁰ was used to assess the importance of various contributions in the perturbation expansion of the He–He interaction.

The QMC equation of state (EOS) for solid neon was computed by Drummond and Needs.²¹⁹ The FNDMC results were found to be in excellent agreement with the experimental EOS and the EOS from literature obtained with a semiempirical pair potential. Newly proposed pair potential from QMC was compatible with the one obtained by CCSD(T). This work again confirms accuracy of QMC for real van der Waals materials.

FNDMC was applied to various solids, including van der Waals ones (Ar, Kr, and Xe) by Shulenburger and Mattsson.¹⁴⁹ The DMC demonstrated predictive behavior for crystal equilibrium volumes and bulk moduli that were in good agreement with experiments.

A challenging problem of Xe crystal melting was studied by combination of FNDMC and thermodynamic integration, by Shulenburger et al.¹⁹² The accuracy of the employed methodology allowed for the indication of potential biases in experiments.

Benali et al. extensively examined Ar dimer, Ar trimer, and solid Ar, Kr, and Xe by FNDMC.⁸⁴ The study of Ar dimer and trimer shown excellent agreement with respect to CCSD(T), while the bulk calculations showed good agreement with the experiment. The results validate the performance of FNDMC for the noble gas systems, both in molecular and condensed forms.

Finally, Clay et al. benchmarked DFT versus QMC in H/He mixtures in order to facilitate development of new functionals for H–He phase diagram.²³⁴

4.3. Water and Ice

Noncovalent interactions in water are among the most studied topics, in part because of water abundance, omnipresence, and importance for biological systems, but also because of anomalous and interesting properties of liquid water. The unusual properties of water mostly result from the specific nature of hydrogen bonds between its molecules.

Water dimer, a prototypical example of hydrogen bonding, was extensively and repeatedly studied by QMC (refs 58, 66, 79, 81, 137, 184, 206, and 241).

However, researchers are more interested in the modeling of bulk water and its anomalous properties. One way of approaching structure and energetics of bulk is through the studies of water clusters with increasing system size. Santra et al. reported on a study of water hexamer isomers.¹⁷⁷ Gillan et al. studied large thermal ensembles and equilibrium structures of small water clusters (H₂O)_n of size $n \leq 6$ by FNDMC and confirmed its benchmark capability by comparison with CCSD(T).⁷⁸ Similar benchmarks on thermal-equilibrium water clusters and bulk water liquid containing up to 64 water molecules were reported by Alfè et al.²⁴² Gillan et al. performed partitioning of total energies of the water hexamer and ice phases (Figure 10) by an expansion in appropriate many-body components with the idea of identifying deficiencies of popular DFT functionals.²²² These studies confirm benchmark capabilities of FNDMC for water and also enabled the detection/correction of particular DFT functional biases. Wang et al.

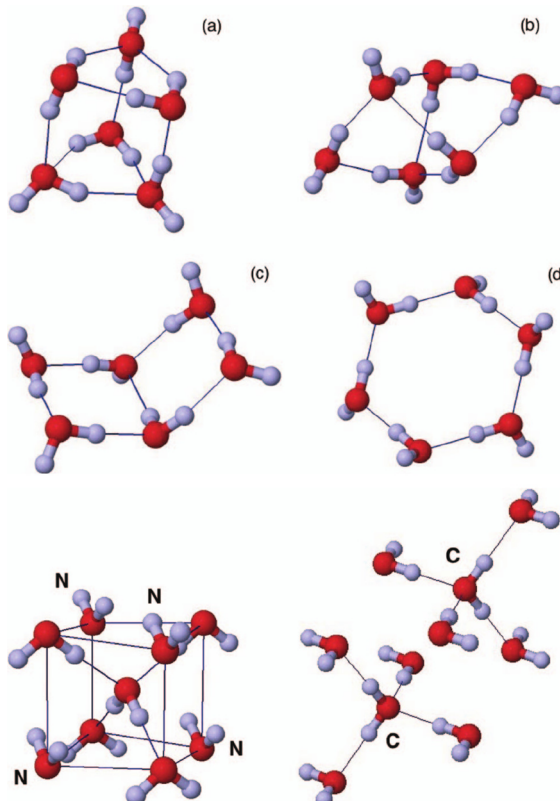


Figure 10. Water hexamer clusters (a–d) and ice crystal structures studied in ref 222. Reprinted with permission from ref 222. Copyright 2013 AIP Publishing LLC.

computed the binding energy of the $(\text{H}_2\text{O})_{16}$ water cluster (Figure 11) by FNDMC. The interaction energy was comparable to the value from MP2.²¹⁰

Another branch of bulk/liquid water research includes explicit consideration of periodicity. Compressed water,²⁴³ bulk water,²⁴⁴ and bulk liquid water²⁴² were studied with the help of QMC methods. A potentially new polytype of ice was predicted on the basis of DMC calculations by Raza et al.²²¹ Santra et al. examined van der Waals and hydrogen bond contributions to the lattice energy of ice at ambient and high pressures and found that at high pressures, the van der Waals contributions are more important than the hydrogen bonding.²²⁰ The stability of ice 0 was examined by Quigley et al. using DFT and QMC to obtain lattice energies that indicated possibility of two competitive phases, ice 0 and ice i.²⁴⁵

Accurate modeling of bulk liquid water at finite temperature requires extensive sampling of its configuration space. For instance, heat of water vaporization was computed by Grossman and Mitas using molecular dynamics coupled with FNDMC.²⁴⁶

Another important and challenging research task is the understanding and prediction of structural and energetic features of solvation processes in water. For example, solvation of methane in water clusters attracted attention for a possible use of methane hydrate as a source of natural gas. Deible et al. studied binding energy of CH_4 in the dodecahedral $(\text{H}_2\text{O})_{20}$ cluster.²⁰² A reference FNDMC study of bulk sI methane hydrate crystal was presented by Cox et al.²⁰¹ The FNDMC benchmarks of CH_4 interacting with water clusters containing up to 20 H_2O molecules were obtained by Gillan et al.⁶⁸ For the CH_4 complex interacting with a single water molecule, an extensive test versus CCSD(T)/CBS on a large ensemble taken from molecular

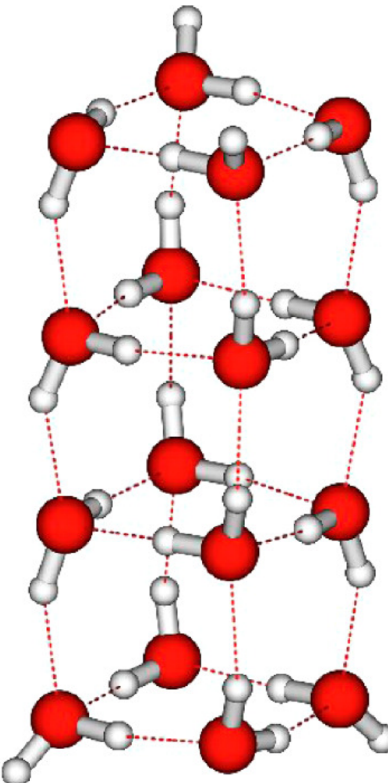


Figure 11. The $(\text{H}_2\text{O})_{16}$ water cluster studied in ref 210. Reprinted from ref 210. Copyright 2013 American Chemical Society.

dynamics proved accuracy of DMC and deviations of up to about 0.15 kcal/mol, distributed around zero (mean 20 μH) were attributed mainly to statistical errors.

To date, a few publications explored interactions of the water molecule with surfaces. These include studies of water on graphene,²⁴⁷ water on $\text{MgO}(100)$,²¹² and water on hexagonal boron nitride (Figure 15).^{160,162}

4.4. Carbon-Based Systems

QMC studies of noncovalent interactions of pure carbon-based molecules and materials, including their interactions with molecules without carbon atoms, are listed in this section.

Benzene dimer is a prototypical system for studies of various types of noncovalent interactions. Depending on the configuration, stacking, or improper hydrogen bonds can contribute to the overall binding. Sorella et al. used advanced QMC techniques to study the face-to-face and parallel displaced configurations of benzene dimer and obtained results with accuracy comparable to the experiment.²⁴⁸ Diedrich et al.⁸¹ analyzed T-shaped and parallel displaced configurations of benzene dimer to test accuracy of FNDMC. Korth et al.⁸² and Dubecký et al.^{66,79} calculated interaction energies of benzene dimer configuration(s) from the benchmark set S22 by FNDMC and compared them to the CCSD(T)/CBS benchmarks.⁵⁴ Azadi and Cohen reported on a QMC study of parallel displaced benzene dimer.²⁴⁹

Interactions of benzene with various small molecules, including hydrogen, methane, oxygen, water, HCN, and ammonia, were studied by Kanai and Grossman using FNDMC.²⁵⁰ Beaudet et al. studied intermolecular potential of benzene- H_2 complex.²⁰⁴ Extensive study of the benzene–water interaction including the benzene–water energy-distance curve was considered by Ma et al.¹⁷⁸ Xu et al. used benzene–water complex in tests of one-particle orbitals.²⁰⁶ A FNDMC

interaction energy of a larger circular polycyclic aromatic hydrocarbon, coronene, interacting with molecular hydrogen, was reported by Kocman et al.²³²

Interaction energy benchmark of water with a small model of graphene surface (3×3) was presented by Ma et al.²⁴⁷ Adsorption of atomic hydrogen on benzene, coronene, and graphene was reported by Ma et al.²¹¹ A study of adsorption of atomic O, F, and H on graphene was published by Hsing et al.²¹⁷

Spanu et al. estimated interlayer binding energy of graphite by QMC and observed good agreement between theory and recent experiment.²⁵¹ Interaction of bilayer graphene was estimated by Mostaani et al.¹⁵⁹ Adsorption and diffusion of intercalated Li in graphite by FNDMC was benchmarked by Ganesh et al.²¹⁴

Interactions of carbon nanotubes with small functional and molecular groups were studied by Cicero et al.²⁵² Kim et al. modeled light-element doped fullerenes useful for hydrogen storage applications.¹⁹⁷

A FNDMC interaction energy of large supra-molecular buckyball catcher host–guest complex ($C_{60}\text{-}C_{60}\text{H}_{28}$) was estimated by Tkatchenko et al.¹⁵⁸

Finally, we note that the anthracene dimerization reaction, where inter- and intramolecular forces are both important, was studied by Grimme et al. using high-level methods of quantum chemistry including QCISD(T) and FNDMC that were in good agreement with each other.¹⁹⁶

4.5. Biomolecular Complexes

An accurate knowledge of interactions in biomolecules is of utmost importance for understanding of their structure and function and high quality calculations have a potential to provide important insights in this area. In addition, modeling of biomolecular structure and dynamics profits from accurate reference values needed for calibration of less demanding quantum chemical, semiempirical, and empirical methods used in molecular dynamics simulations. Typical size of biomolecules is, however, often relatively large and out of reach of the current WFT benchmark methods. Therefore, reference calculations on biomolecular complexes are challenging mainly because of the size that is required for obtaining useful results. For these types of problems, QMC calculations may offer a significant advantage.

QMC methods were applied to biomolecular systems of intermediate and large sizes (see Figure 12 and Figure 13 for examples). Korth et al. in their pioneering work benchmarked

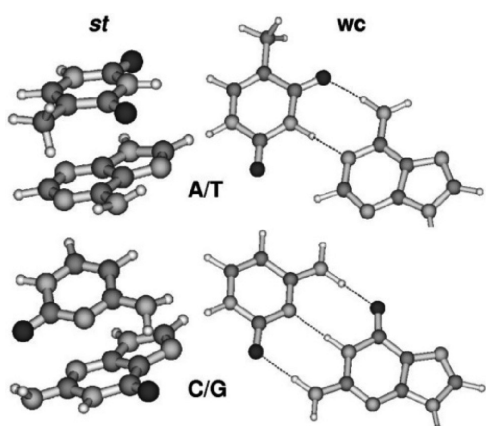


Figure 12. Structures of DNA base pairs, studied by Korth et al.,⁸² include stacked and Watson–Crick adenine-thymine and stacked and Watson–Crick cytosine-guanine. Reprinted with permission from ref 82. Copyright 2008 American Chemical Society.

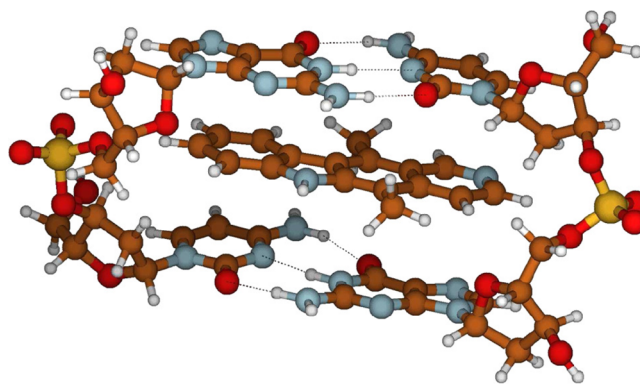


Figure 13. Interaction strength of a large DNA fragment intercalated with ellipticine drug was quantified by Benali et al. Reprinted from ref 84. Copyright 2014 American Chemical Society.

FNDMC versus CCSD(T)/CBS on a large set of 22 molecules (S22), including biomolecular ones, and performed large-scale calculations to obtain interaction energies of adenine-thymine and cytosine-guanine base pairs.⁸²

A benchmark FNDMC interaction energy of a large supramolecular host–guest complex, glycine anhydride interacting with amide macrocycle was calculated by Tkatchenko et al.¹⁵⁸

Interaction of adenine-thymine step in B-DNA was estimated by FNDMC in the work of Hongo et al.¹⁹¹

Benali et al. presented a FNDMC estimate of interaction energy for the fragment of DNA intercalated with anticancer drug, ellipticine (Figure 13).⁸⁴

4.6. Host–Guest Complexes

A benchmark FNDMC interaction energies of supramolecular host–guest complexes, buckyball catcher complex, and glycine anhydride interacting with amide macrocycle were reported by Tkatchenko et al.,¹⁵⁸ and subsequently, FNDMC benchmarks were presented for a larger set of six large host–guest complexes (Figure 14) by Ambrosetti et al.⁸³

Benali et al. obtained a FNDMC estimate of the interaction energy for the host–guest complex composed of DNA fragment as a host and ellipticine molecule as a guest (Figure 13).⁸⁴

4.7. Small Molecular Complexes

Molecular complexes may be sorted according to the dominant type of interaction to the following classes: hydrogen-bound, dispersion bound, mixed (containing similar contributions of hydrogen-bonding and dispersion), charged, ionic, and complexes containing metals. We list here papers studying small complexes according to these criteria.

Small complexes with hydrogen bonding: water dimer,^{58,66,79,81,137,184,206,241} ammonia dimer,⁸¹ and HF dimer.^{58,66,79}

Dispersion bound: methane dimer,^{66,79,81,253} benzene dimer,^{66,81,248,249} benzene–H₂,²⁰⁴ benzene with hydrogen, and methane.²⁵⁰

Mixed complexes: methane–water,⁶⁸ benzene–water,^{66,79,178,206,250} benzene–ammonia,²⁵⁰ benzene–oxygen and benzene–HCN,²⁵⁰ and BN-doped benzene–water.⁶⁷

Ionic complexes: thiophene–Li.^{179,254}

Charged complexes: triazine–NO₃⁻¹⁹⁹ and cationic vanadium–benzene.^{255,256}

Metal-containing: neutral and cationic vanadium–benzene,^{255,256} cobalt–benzene,²⁵⁶ and platinum–benzene.²⁵⁷

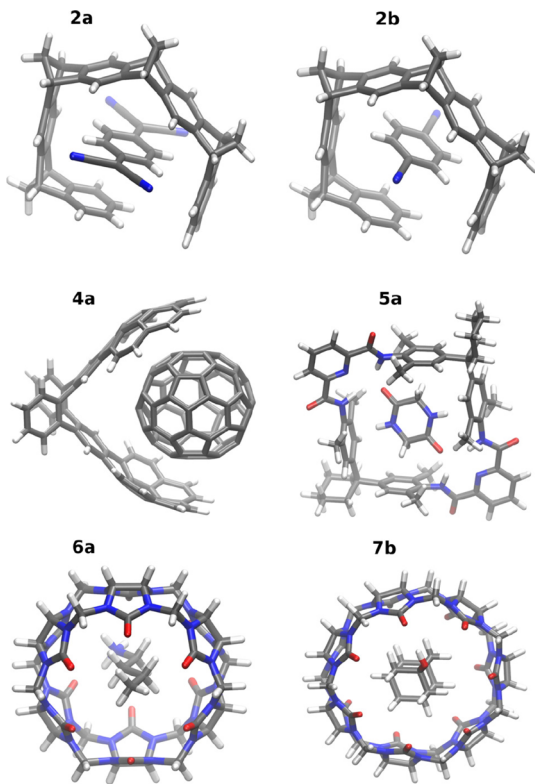


Figure 14. Set of supramolecular complexes considered in benchmark FNDMC calculations by Ambrosetti et al. Reprinted from ref 83. Copyright 2014 American Chemical Society.

Published FNDMC studies of larger benchmark molecular sets include S22,⁸² subset of S22,^{66,79} and a set of 24 complexes A24.^{88,79}

4.8. Nanomaterials

Predictive capabilities of QMC have been used in a number of studies in nanomaterials research. The published work includes interactions of carbon nanotubes with small molecules,²⁵² and NO_2 ,¹⁸⁷ boron- and beryllium-doped fullerenes with potential hydrogen storage capabilities,¹⁹⁷ studies of water–graphene²⁴⁷ and water–hexagonal boron nitride interactions (Figure 15),^{160,161} or van der Waals interactions in a boron nitride

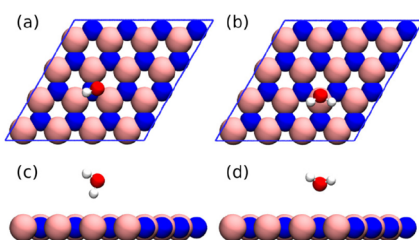


Figure 15. Model of hexagonal boron nitride surface interacting with a water molecule. Reprinted with permission from ref 160. Copyright 2015 AIP Publishing LLC.

bilayer²⁵⁸ and bilayer graphene.¹⁵⁹ Furthermore, Drummond and Needs explored van der Waals interactions in model metallic wires^{259,266} and sheets,²⁶⁶ that mimic one-dimensional (1D) and 2D materials such as carbon nanotubes and graphene.

4.9. Crystals and Surfaces

In addition to noble gas crystals (section 4.2) and bulk water/ice (section 4.3), QMC combined with periodic boundary conditions has been used to study many other systems: H_2 on Si(001) surface,²⁶⁰ interactions of carbon nanotubes with functional groups,²⁵² graphite,²⁵¹ molecular polymorphism of para-diiodobenzene crystal (Figure 16),^{193,261} water on gra-

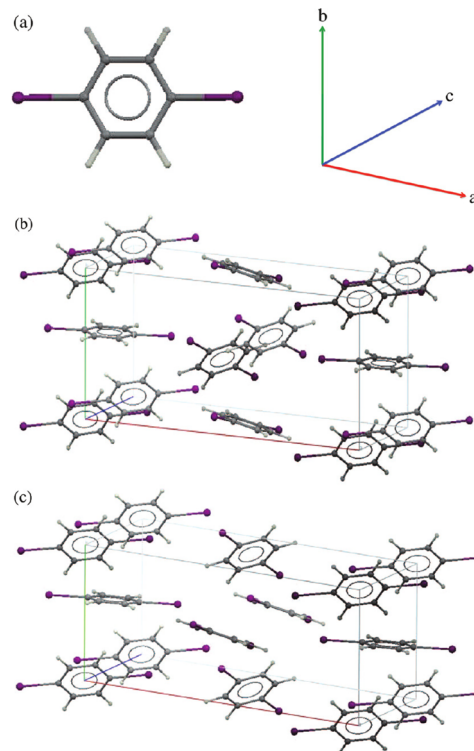


Figure 16. (a) Chemical structure of the para-diiodobenzene molecule and lattice vector labeling, (b) crystal structure of R phase, and (c) crystal structure of the β phase. Reprinted from ref 261. Copyright 2010 American Chemical Society.

phene,²⁴⁷ water on the $\text{MgO}(100)$ surface,²¹² methane hydrate,²⁰¹ interactions of graphite with lithium,²¹⁴ water on hexagonal boron nitride (Figure 15),¹⁶⁰ and van der Waals interactions in a boron nitride bilayer²⁵⁸ and bilayer graphene.¹⁵⁹

4.10. Open-Shell and Multireference Complexes

Accurate description of weak bonding in beryllium dimer, that has a significant nondynamical correlation component, is a challenging task.^{262,263} It has been shown that FNDMC can reasonably describe this small but nontrivial bonding,^{130,189,190,264} although some care must be devoted to the construction of Ψ_T .^{190,264}

Interaction energy of O_2 interacting with a benzene molecule was estimated by Kanai and Grossman using FNDMC with single determinant trial wave functions.²⁵⁰

Hsing et al. studied adsorption of hydrogen, oxygen, and fluorine adatoms by FNDMC.

QMC methods were also applied to noncovalent interactions in metal–benzene complexes with a pronounced open-shell character. These include neutral and cationic vanadium–benzene,^{255,256} cobalt–benzene,²⁵⁶ and platinum–benzene²⁵⁷ complexes.

4.11. Fundamental Insight and Theory

Caffarel and Hess introduced perturbation QMC, a method able to evaluate Rayleigh–Schrödinger perturbation theory at energy order with intermolecular interactions as a perturbation²⁶⁵ and applied it to the He dimer.^{240,265}

Drummond and Needs explored van der Waals interactions in model metallic wires and sheets.^{259,266}

Gurtubay et al. estimated dipole moments of water molecule and water dimer by QMC methods.¹³⁷

Sterpone et al. optimized Jastrow correlated single determinant geminal wave functions and used their terms to quantify contribution of dispersion forces to the interaction energy of water dimer. The value of -1.5 ± 0.2 kcal/mol²⁴¹ was in good agreement with the value of -1.75 kcal/mol from SAPT.⁶⁴

Kanai and Grossman²⁵⁰ used reptation QMC to calculate the reduced density gradient and used it to understand shortcomings of existing xc functionals in description of noncovalent interactions.

5. DISCUSSION AND CHALLENGES

It is reasonable to assume that an explicit construction of exact eigenstate(s) for a large interacting quantum system is both unnecessary and not really useful. What is really “only” needed is the necessary amount of information that enables evaluations of accurate expectation values (e.g., energy differences and other quantities of interest within a desired error margin). This is in fact the basic premise of the reductionism paradigm that underlies a vast number of methods based on mean-fields, DFT, reduced density matrices,^{268–270} etc. The challenge comes from the fact that the reduced quantity is actually a very complicated object since all the many-body effects have been folded into it during the reduction (for example, by integrating over $(N-2)$ particles when getting the two-body density matrix). However, this is in general a very difficult task due to its inverse nature: one wants to reconstruct correlations from the particles that are already integrated out. Advanced methods based on density matrix renormalization^{271–273} and other renormalization group methods or sophisticated perturbation approaches try to address exactly this critical issue by carefully guiding the reduction in an appropriate and presumably efficient manner. However, beyond a certain level the systematic improvements of reduced quantities often becomes very difficult, sometimes perhaps almost as difficult as solving the full many-body problem in the first place.

In this respect, QMC appears to be a unique methodology that combines known analytical insights and direct constructions with the robustness of the stochastic methods in order to capture the many-body effects efficiently. It seems that this combination offers somewhat of a sweet spot between the fully explicit and the fully reduced descriptions. In particular, the uninteresting and heavy load of reducing (i.e., calculating expectation values) is left to the machine.

The value of the QMC method comes also from its new insights that reveal the nature of quantum correlations that are stimulating for correlated wave function methods in general. In particular, (i) stochastic sampling is carried out from a complete basis, and the extent of sampling is determined automatically by the desired error bar, largely avoiding thus the basis set issues; (ii) to the leading order, the explicit inclusion of exact nonanalytical behavior, such as electron–electron cusps, eliminates another issue that is difficult in many other approaches; and (iii) in addition, the correlation factor captures the smooth, medium-,

and long-range correlations with remarkable efficiency, with just a few to a few tens of variational parameters.

On the other hand, as expected, QMC has its own limitations and challenges.

The key challenge that has a long history and that has to do with the fundamental and infamous Fermion sign problem can be formulated also as a construction of an optimal effective Hamiltonian. The actual Hamiltonian that is solved exactly by the fixed-node DMC can be written as

$$H_{\text{FN}} = H + V_{\infty}(\Gamma) \quad (17)$$

where Γ is the location of the nodal hypersurface and $V_{\infty}(\Gamma)$ is an infinite barrier at this subset of configurations. Improvement of $V_{\infty}(\Gamma)$ is done indirectly through more accurate trial functions, and it is therefore important to understand the sources of the nodal errors. As described above, the fixed-node bias grows with the electronic density as well as with the complexity of the bonds.¹²² This finding has implications also for noncovalent systems since dispersion interactions result in low densities and mainly σ -like character of single-reference bonds, hence the fixed-node errors are much less pronounced in energy differences. However, this finding has a significant importance also for other electronic structure problems and possibly beyond. Clearly, these arguments need to be further refined and quantified so that much remains to be done in this direction.

Another “technical” issue of importance is the construction and testing of accurate ECPs: since QMC can provide benchmark accuracy for many systems, the quality of ECPs for heavier elements becomes crucial. In particular, new opportunities would open up with ECPs that would enable valence-only calculations with an accuracy target, say, 0.1 kcal/mol (≈ 0.005 eV) or so for energy differences. Furthermore, overall applicability of QMC methods could be significantly enhanced with more systematic benchmarking, testing, and providing data sets of calculations for a broad use.

Perhaps one of the greatest challenges is better understanding of errors related to current QMC procedures. So far most of the calculations focused on energy differences such as cohesion, gaps, and similar quantities that are larger than 0.1 eV or so, rather than on tiny differences important for intermolecular bonding. Even though some sources of errors have been already identified, it is still not fully understood to what extent they are systematic, how they scale with the system size, and what are the best ways of reducing them. In addition, it is still possible that more sources of errors will be uncovered. This state of the matter is strikingly different from the mainstream WFT, where sources of errors are very well mapped out and many solutions exist that may be routinely applied. Much more detailed work will be necessary to achieve this level of routine with the QMC methods.

One of the open challenges is also optimization of the QMC codes and development of new fast algorithms. Whereas mainstream methods and codes were optimized for performance over many decades, both on the side of more efficient programming and method development, at present the QMC codes are mostly basic research tools. Obviously, this is an opportunity for future as it is likely that QMC codes may become more efficient once they become more widely used.

6. CONCLUSIONS

We presented basic notions of electronic structure QMC methods and a comprehensive overview of methodological and application aspects of QMC for systems with noncovalent interactions.

Advantages such as efficient treatment of dynamic correlations essential for accurate description of noncovalent interactions, low-order polynomial scaling allowing applications to much larger molecular systems than possible within the current mainstream WFT approaches, favorable parallelism of algorithms suited for modern high-performance parallel supercomputers, or straightforward treatment of periodicity make QMC methodology an attractive choice for future development.

We envision an increase in the number of QMC applications to nanomaterials, biomolecular, and other large noncovalent complexes in upcoming years. However, expansion of QMC applicability calls for further systematic investigation of errors, approximations, and limitations inherent to QMC approaches, which are not yet fully understood. The broad community of potential users would benefit from more robust and reliable computational protocols, user-friendly interfaces, and faster codes.

AUTHOR INFORMATION

Corresponding Authors

*E-mail: matus.dubecky@osu.cz.

*E-mail: lmitas@ncsu.edu.

Notes

The authors declare no competing financial interest.

Biographies

Matúš Dubecký is a research scientist at the University of Ostrava in Czech Republic. He pursued a Ph.D. study at the Nanyang Technological University in Singapore (with Haibin Su) and Institute of Physics, Slovak Academy of Sciences in Bratislava (Slovakia, with Ivan Štich) and obtained his Ph.D. in solid state physics at the Comenius University in Bratislava. He spent three years as a postdoc at the Regional Centre of Advanced Technologies and Materials, Palacký University Olomouc in Czech Republic (with Michal Otyepka), where he studied noncovalent interactions by QMC. He is interested in development and application of quantum Monte Carlo methods to challenging electronic structure problems, including noncovalent interactions and strongly correlated systems.

Lubos Mitas obtained his Ph.D. ("C.Sc.") degree at the Institute of Physics of Slovak Academy of Sciences, Bratislava, Slovakia, in 1989. He spent his postdoctoral years with D. M. Ceperley and R. M. Martin at the University of Illinois in Urbana-Champaign. He was awarded several Fellowships during his career such as from ICTP (Trieste, Italy, 1988), NSERC (Ottawa, Canada, 1992), and NSF (US, 1992). At present, he is a Professor at the Department of Physics, North Carolina State University, Raleigh. His main research interests are in computational physics, electronic structure, quantum Monte Carlo (QMC), and applied mathematics. He is known for pioneering electronic structure QMC calculations with pseudopotentials for molecular, cluster, and solid systems, use of pfaffian wave functions in QMC, analysis of nodal topologies of Fermionic wave functions, and other accomplishments. He is a Fellow of the American Physical Society from 2010.

Petr Jurečka obtained his Ph.D. from the Charles University in Prague and the Institute of Organic Chemistry and Biochemistry in 2004 (with Pavel Hobza). He did his postdoctoral study with Professor D. R. Salahub at the University of Calgary, Canada. He is currently an Associate Professor at the Department of Physical Chemistry at the Palacký University in Olomouc. His main interests are related to the empirical force field development for nucleic acids, simulations of conformational equilibria in RNA and DNA, theoretical description of

noncovalent interactions in biomolecules and nanomaterials, highly accurate quantum chemistry calculations, and density functional theory.

ACKNOWLEDGMENTS

Support from the Ministry of Education, Youth and Sports of the Czech Republic (project no. LO1305) is gratefully acknowledged. M.D. was in part funded by the Palacky University institutional support. L.M. gratefully acknowledges support by the NSF grant DMR-1410639 and by XSEDE computer time allocation at TACC.

REFERENCES

- (1) Autumn, K.; Sitti, M.; Liang, Y. A.; Peattie, A. M.; Kenny, T. W.; Fearing, R.; Israelachvili, J. N.; Hansen, W. R.; Sponberg, S.; Full, R. J. Evidence for van der Waals adhesion in gecko setae. *Proc. Natl. Acad. Sci. U. S. A.* **2002**, *99*, 12252–12256.
- (2) Riley, K. E.; Hobza, P. On the Importance and Origin of Aromatic Interactions in Chemistry and Biodisciplines. *Acc. Chem. Res.* **2013**, *46*, 927–936.
- (3) Grimme, S. Supramolecular Binding Thermodynamics by Dispersion-Corrected Density Functional Theory. *Chem. - Eur. J.* **2012**, *18*, 9955–9964.
- (4) Juríček, M.; Strutt, N. L.; Barnes, J. C.; Butterfield, A. M.; Dale, E. J.; Baldridge, K. K.; Stoddart, J. F.; Siegel, J. S. Induced-fit catalysis of corannulene bowl-to-bowl inversion. *Nat. Chem.* **2014**, *6*, 222–228.
- (5) Liu, W.; Tkatchenko, A.; Scheffler, M. Modeling Adsorption and Reactions of Organic Molecules at Metal Surfaces. *Acc. Chem. Res.* **2014**, *47*, 3369–3377.
- (6) Kronik, L.; Tkatchenko, A. Understanding Molecular Crystals with Dispersion-Inclusive Density Functional Theory: Pairwise Corrections and Beyond. *Acc. Chem. Res.* **2014**, *47*, 3208–3216.
- (7) Šponer, J.; Šponer, J. E.; Mládek, A.; Jurečka, P.; Banáš, P.; Otyepka, M. Nature and Magnitude of Aromatic Base Stacking in DNA and RNA: Quantum Chemistry, Molecular Mechanics, and Experiment. *Biopolymers* **2013**, *99*, 978.
- (8) Riley, K. E.; Hobza, P. Noncovalent interactions in biochemistry. *Comp. Mol. Sci.* **2011**, *1*, 3–17.
- (9) Murthy, P. S. Molecular Handshake: Recognition through Weak Noncovalent Interactions. *J. Chem. Educ.* **2006**, *83*, 1010.
- (10) Rubbiani, R.; Can, S.; Kitanovic, I.; Alborzinia, H.; Stefanopoulou, M.; Kokoschka, M.; Mönchgesang, S.; Sheldrick, W. S.; Wölf, S.; Ott, I. Comparative in Vitro Evaluation of N-Heterocyclic Carbene Gold(I) Complexes of the Benzimidazolylidene Type. *J. Med. Chem.* **2011**, *54*, 8646–8657.
- (11) Meyer, A.; Bagowski, C. P.; Kokoschka, M.; Stefanopoulou, M.; Alborzinia, H.; Can, S.; Vlecken, D. H.; Sheldrick, W. S.; Wölf, S.; Ott, I. On the biological properties of alkynyl phosphine gold(I) complexes. *Angew. Chem., Int. Ed.* **2012**, *51*, 8895–8899.
- (12) Beno, B. R.; Yeung, K.-S.; Bartberger, M. D.; Pennington, L. D.; Meanwell, N. A. Survey of the Role of Noncovalent Sulfur Interactions in Drug Design. *J. Med. Chem.* **2015**, *58*, 4383–4438.
- (13) Riley, K. E.; Pitoňák, M.; Jurečka, P.; Hobza, P. Stabilization and Structure Calculations for Noncovalent Interactions in Extended Molecular Systems Based on Wave Function and Density Functional Theories. *Chem. Rev.* **2010**, *110*, 5023–5063.
- (14) Georgakilas, V.; Otyepka, M.; Bourlins, A. B.; Chandra, V.; Kim, N.; Kemp, K. C.; Hobza, P.; Zbořil, R.; Kim, K. S. Functionalization of Graphene: Covalent and Non-Covalent Approaches, Derivatives and Applications. *Chem. Rev.* **2012**, *112*, 6156–6214.
- (15) DiStasio, R. A.; Gobre, V. V.; Tkatchenko, A. Many-body van der Waals interactions in molecules and condensed matter. *J. Phys.: Condens. Matter* **2014**, *26*, 213202.
- (16) Chalański, G.; Szczęśniak, M. M. State of the Art and Challenges of the ab Initio Theory of Intermolecular Interactions. *Chem. Rev.* **2000**, *100*, 4227–4252.
- (17) Pykal, M.; Jurečka, P.; Karlický, F.; Otyepka, M. Modelling of graphene functionalization. *Phys. Chem. Chem. Phys.* **2016**, *18*, 6351.

- (18) Hobza, P.; Müller-Dethlefs, K. *Non-Covalent Interactions*; RSC Theoretical and Computational Chemistry Series; RSC Publishing, 2010.
- (19) Lazar, P.; Karlický, F.; Jurečka, P.; Kocman, M.; Otyepková, E.; Šafářová, K.; Otyepka, M. Adsorption of Small Organic Molecules on Graphene. *J. Am. Chem. Soc.* **2013**, *135*, 6372–6377.
- (20) Karlický, F.; Otyepková, E.; Banáš, P.; Lazar, P.; Kocman, M.; Otyepka, M. Interplay between Ethanol Adsorption to High-Energy Sites and Clustering on Graphene and Graphite Alters the Measured Isosteric Adsorption Enthalpies. *J. Phys. Chem. C* **2015**, *119*, 20535–20543.
- (21) Stone, A. J. *The Theory of Intermolecular Forces*; Calerdon Press: Oxford, 2002.
- (22) Jeziorski, B.; Moszynski, R.; Szalewicz, K. Perturbation Theory Approach to Intermolecular Potential Energy Surfaces of van der Waals Complexes. *Chem. Rev.* **1994**, *94*, 1887–1930.
- (23) Boehr, D. D.; Nussinov, R.; Wright, P. E. The role of dynamic conformational ensembles in biomolecular recognition. *Nat. Chem. Biol.* **2009**, *5*, 789–796.
- (24) Risthaus, T.; Grimme, S. Benchmarking of London Dispersion-Accounting Density Functional Theory Methods on Very Large Molecular Complexes. *J. Chem. Theory Comput.* **2013**, *9*, 1580–1591.
- (25) Sure, R.; Grimme, S. Comprehensive Benchmark of Association (Free) Energies of Realistic Host-Guest Complexes. *J. Chem. Theory Comput.* **2015**, *11*, 3785–3801.
- (26) Cao, L.; Škalamera, D.; Zavalij, P. Y.; Hostaš, J.; Hobza, P.; Mlinarić-Majerski, K.; Glaser, R.; Isaacs, L. Influence of hydrophobic residues on the binding of CB[7] toward diammonium ions of common ammonium···ammonium distance. *Org. Biomol. Chem.* **2015**, *13*, 6249–6254.
- (27) Lee, J.; Sorescu, D. C.; Deng, X.; Jordan, K. D. Water Chain Formation on TiO₂ Rutile(110). *J. Phys. Chem. Lett.* **2013**, *4*, 53–57.
- (28) Bartels, L. Tailoring molecular layers at metal surfaces. *Nat. Chem.* **2010**, *2*, 87–95.
- (29) Auwärter, W.; Écija, D.; Klappenberger, F.; Barth, J. V. Porphyrins at interfaces. *Nat. Chem.* **2015**, *7*, 105–120.
- (30) Vítek, A.; Ofiala, A.; Kalus, R. Thermodynamics of water clusters under high pressures. A case study for (H₂O)₁₅ and (H₂O)₁₅CH₄. *Phys. Chem. Chem. Phys.* **2012**, *14*, 15509–15519.
- (31) Chattoraj, J.; Risthaus, T.; Rubner, O.; Heuer, A.; Grimme, S. A multi-scale approach to characterize pure CH₄, CF₄, and CH₄/CF₄ mixtures. *J. Chem. Phys.* **2015**, *142*, 164508.
- (32) Řezáč, J.; Fanfrlík, J.; Salahub, D.; Hobza, P. Semiempirical Quantum Chemical PM6 Method Augmented by Dispersion and H-Bonding Correction Terms Reliably Describes Various Types of Noncovalent Complexes. *J. Chem. Theory Comput.* **2009**, *5*, 1749–1760.
- (33) Brandenburg, J. G.; Hochheim, M.; Bredow, T.; Grimme, S. Low-Cost Quantum Chemical Methods for Noncovalent Interactions. *J. Phys. Chem. Lett.* **2014**, *5*, 4275–4284.
- (34) Grimme, S.; Brandenburg, J. G.; Bannwarth, C.; Hansen, A. Consistent structures and interactions by density functional theory with small atomic orbital basis sets. *J. Chem. Phys.* **2015**, *143*, 054107.
- (35) Grimme, S. Density functional theory with London dispersion corrections. *WIREs* **2011**, *1*, 211–228.
- (36) Waller, M. P.; Kruse, H.; Muck-Lichtenfeld, C.; Grimme, S. Investigating inclusion complexes using quantum chemical methods. *Chem. Soc. Rev.* **2012**, *41*, 3119–3128.
- (37) Řezáč, J.; Hobza, P. Benchmark Calculations of Interaction Energies in Noncovalent Complexes and Their Applications. *Chem. Rev.* **2016**, DOI: [10.1021/acs.chemrev.5b00526](https://doi.org/10.1021/acs.chemrev.5b00526).
- (38) Beran, G. J. O. Modeling Polymorphic Molecular Crystals with Electronic Structure Theory. *Chem. Rev.* **2016**, DOI: [10.1021/acs.chemrev.5b00648](https://doi.org/10.1021/acs.chemrev.5b00648).
- (39) Cohen, A. J.; Mori-Sánchez, P.; Yang, W. Challenges for Density Functional Theory. *Chem. Rev.* **2012**, *112*, 289–320.
- (40) Thiel, W. Semiempirical quantum-chemical methods. *WIREs Comput. Mol. Sci.* **2014**, *4*, 145–157.
- (41) Grimme, S. A. General Quantum Mechanically Derived Force Field (QMDF) for Molecules and Condensed Phase Simulations. *J. Chem. Theory Comput.* **2014**, *10*, 4497–4514.
- (42) Šponer, J.; Banáš, P.; Jurečka, P.; Zgarbová, M.; Kührová, P.; Havrlá, M.; Krepl, M.; Stadlbauer, P.; Otyepka, M. Molecular Dynamics Simulations of Nucleic Acids. From Tetranucleotides to the Ribosome. *J. Phys. Chem. Lett.* **2014**, *5*, 1771–1782.
- (43) Schuurman, M. S.; Muir, S. R.; Allen, W. D.; Schaefer, H. F., III. Toward subchemical accuracy in computational thermochemistry: Focal point analysis of the heat of formation of NCO and [H,N,C,O] isomers. *J. Chem. Phys.* **2004**, *120*, 11586–11599.
- (44) Řezáč, J.; Hobza, P. Describing Noncovalent Interactions beyond the Common Approximations: How Accurate Is the "Gold Standard," CCSD(T) at the Complete Basis Set Limit? *J. Chem. Theory Comput.* **2013**, *9*, 2151–2155.
- (45) Risthaus, T.; Grimme, S. Benchmarking of London Dispersion-Accounting Density Functional Theory Methods on Very Large Molecular Complexes. *J. Chem. Theory Comput.* **2013**, *9*, 1580–1591.
- (46) Iliáš, M.; Kellö, V.; Urban, M. Relativistic Effects in Atomic and Molecular Properties. *Acta Phys. Slovaca* **2010**, *60*, 259–391.
- (47) Čížek, J. On the Correlation Problem in Atomic and Molecular Systems. Calculation of Wavefunction Components in Ursell-Type Expansion Using Quantum-Field Theoretical Methods. *J. Chem. Phys.* **1966**, *45*, 4256.
- (48) Čížek, J. *Adv. Chem. Phys.* **1969**, *14*, 35.
- (49) Paldus, J.; Čížek, J.; Shavitt, I. Correlation Problems in Atomic and Molecular Systems. IV. Extended Coupled-Pair Many-Electron Theory and Its Application to the BH₃ Molecule. *Phys. Rev. A: At., Mol., Opt. Phys.* **1972**, *5*, 50.
- (50) Raghavachari, K.; Trucks, G. W.; Pople, J. A.; Head-Gordon, M. A fifth-order perturbation comparison of electron correlation theories. *Chem. Phys. Lett.* **1989**, *157*, 479–483.
- (51) Bartlett, R. J.; Watts, S. A.; Kucharski, J. D.; Noga, J. Non-iterative fifth-order triple and quadruple excitation energy corrections in correlated methods. *Chem. Phys. Lett.* **1990**, *165*, 513–522.
- (52) Scuseria, G. E.; Lee, T. J. Comparison of coupled-cluster methods which include the effects of triple excitations. *J. Chem. Phys.* **1990**, *93*, 5851–5855.
- (53) Crawford, T. D.; Stanton, J. F. Investigation of an asymmetric triple-excitation correction for coupled cluster energies. *Int. J. Quantum Chem.* **1998**, *70*, 601–611.
- (54) Jurečka, P.; Šponer, J.; Černý, J.; Hobza, P. Benchmark database of accurate (MP2 and CCSD(T) complete basis set limit) interaction energies of small model complexes, DNA base pairs, and amino acid pairs. *Phys. Chem. Chem. Phys.* **2006**, *8*, 1985–1993.
- (55) Podeszwa, R.; Patkowski, K.; Szalewicz, K. Improved interaction energy benchmarks for dimers of biological relevance. *Phys. Chem. Chem. Phys.* **2010**, *12*, 5974–5979.
- (56) Takatani, T.; Hohenstein, E. G.; Malagoli, M.; Marshall, M. S.; Sherrill, C. D. Basis set consistent revision of the S22 test set of noncovalent interaction energies. *J. Chem. Phys.* **2010**, *132*, 144104.
- (57) Ranasinghe, D. S.; Petersson, G. A. CCSD(T)/CBS atomic and molecular benchmarks for H through Ar. *J. Chem. Phys.* **2013**, *138*, 144104.
- (58) Řezáč, J.; Dubecký, M.; Jurečka, P.; Hobza, P. Extensions and applications of the A24 data set of accurate interaction energies. *Phys. Chem. Chem. Phys.* **2015**, *17*, 19268–19277.
- (59) Šimová, L.; Řezáč, J.; Hobza, P. Convergence of the Interaction Energies in Noncovalent Complexes in the Coupled-Cluster Methods Up to Full Configuration Interaction. *J. Chem. Theory Comput.* **2013**, *9*, 3420–3428.
- (60) Smith, D. G. A.; Jankowski, P.; Slawik, M.; Witek, H. A.; Patkowski, K. Basis Set Convergence of the Post-CCSD(T) Contribution to Noncovalent Interaction Energies. *J. Chem. Theory Comput.* **2014**, *10*, 3140–3150.
- (61) Řezáč, J.; Hobza, P. Ab Initio Quantum Mechanical Description of Noncovalent Interactions at Its Limits: Approaching the Experimental Dissociation Energy of the HF Dimer. *J. Chem. Theory Comput.* **2014**, *10*, 3066–3073.

- (62) Hohenstein, E. G.; Sherrill, C. D. Wavefunction methods for noncovalent interactions. *WIREs Comput. Mol. Sci.* **2012**, *2*, 304–326.
- (63) Szalewicz, K. Symmetry-adapted perturbation theory of intermolecular forces. *WIREs Comput. Mol. Sci.* **2012**, *2*, 254–272.
- (64) Misquitta, A. J.; Podeszwa, R.; Jeziorski, B.; Szalewicz, K. Intermolecular potentials based on symmetry-adapted perturbation theory with dispersion energies from time-dependent density-functional calculations. *J. Chem. Phys.* **2005**, *123*, 214103.
- (65) Hesselmann, A.; Jansen, G.; Schütz, M. Comprehensive Benchmark of Association (Free) Energies of Realistic Host-Guest Complexes. *J. Chem. Phys.* **2005**, *122*, 014103.
- (66) Dubeczký, M.; Jurečka, P.; Derian, R.; Hobza, P.; Otyepka, M.; Mitas, L. Quantum Monte Carlo Methods Describe Noncovalent Interactions with Subchemical Accuracy. *J. Chem. Theory Comput.* **2013**, *9*, 4287–4292.
- (67) Al-Hamdani, Y. S.; Alfè, D.; von Lilienfeld, O. A.; Michaelides, A. Water on BN doped benzene: A hard test for exchange-correlation functionals and the impact of exact exchange on weak binding. *J. Chem. Phys.* **2014**, *141*, 18CS30.
- (68) Gillan, M. J.; Alfè, D.; Manby, F. R. Energy benchmarks for methane-water systems from quantum Monte Carlo and second-order Møller-Plesset calculations. *J. Chem. Phys.* **2015**, *143*, 102812.
- (69) Deyonker, N. J.; Cundari, T. R.; Wilson, A. K. The correlation consistent composite approach (ccCA): An alternative to the Gaussian-n methods. *J. Chem. Phys.* **2006**, *124*, 114104.
- (70) Jurečka, P.; Hobza, P. True Stabilization Energies for the Optimal Planar Hydrogen-Bonded and Stacked Structures of GuanineCytosine, AdenineThymine, and Their 9- and 1-Methyl Derivatives: Complete Basis Set Calculations at the MP2 and CCSD(T) Levels and Comparison with Experiment. *J. Am. Chem. Soc.* **2003**, *125*, 15608–15613.
- (71) Demovičová, L.; Hobza, P.; Řežáč, J. Evaluation of composite schemes for CCSDT(Q) calculations of interaction energies of noncovalent complexes. *Phys. Chem. Chem. Phys.* **2014**, *16*, 19115–19121.
- (72) Janowski, T.; Ford, A. R.; Pulay, P. Accurate correlated calculation of the intermolecular potential surface in the coronene dimer. *Mol. Phys.* **2010**, *108*, 249–257.
- (73) Riplinger, C.; Sandhoefer, C.; Hansen, F.; Neese, A. Natural triple excitations in local coupled cluster calculations with pair natural orbitals. *J. Chem. Phys.* **2013**, *139*, 134101.
- (74) Schütz, M.; Masur, O.; Usvyat, D. Efficient and accurate treatment of weak pairs in local CCSD(T) calculations. II. Beyond the ring approximation. *J. Chem. Phys.* **2014**, *140*, 244107.
- (75) Yang, J.; Hu, W.; Usvyat, D.; Matthews, D.; Schütz, M.; Chan, G.-L. Ab initio determination of the crystalline benzene lattice energy to sub-kilojoule/mol accuracy. *Science* **2014**, *345*, 640–643.
- (76) Pittner, J. Continuous transition between Brillouin-Wigner and Rayleigh-Schrödinger perturbation theory, generalized Bloch equation, and Hilbert space multireference coupled cluster. *J. Chem. Phys.* **2003**, *118*, 10876–10889.
- (77) Evangelista, F. A.; Allen, W. D.; Schaefer, H. F. Coupling Term Derivation and General Implementation of State-Specific Multi-reference Coupled Cluster Theories. *J. Chem. Phys.* **2007**, *127*, 024102.
- (78) Gillan, M. J.; Manby, F. R.; Towler, M. D.; Alfè, D. Assessing the accuracy of quantum Monte Carlo and density functional theory for energetics of small water clusters. *J. Chem. Phys.* **2012**, *136*, 244105.
- (79) Dubeczký, M.; Derian, R.; Jurečka, P.; Hobza, P.; Otyepka, M.; Mitas, L. Quantum Monte Carlo for noncovalent interactions: an efficient protocol attaining benchmark accuracy. *Phys. Chem. Chem. Phys.* **2014**, *16*, 20915–20923.
- (80) Mella, M.; Anderson, J. B. Intermolecular forces and fixed-node diffusion Monte Carlo: A brute force test of accuracies for He_2 and He-LiH . *J. Chem. Phys.* **2003**, *119*, 8225–8228.
- (81) Diedrich, C.; Lüchow, A.; Grimme, S. Weak intermolecular interactions calculated with diffusion Monte Carlo. *J. Chem. Phys.* **2005**, *123*, 184106.
- (82) Korth, M.; Lüchow, A.; Grimme, S. Toward the Exact Solution of the Electronic Schrödinger Equation for Noncovalent Molecular Interactions: Worldwide Distributed Quantum Monte Carlo Calculations. *J. Phys. Chem. A* **2008**, *112*, 2104–2109.
- (83) Ambrosetti, A.; Alfè, D.; DiStasio, R. A., Jr.; Tkatchenko, A. Hard Numbers for Large Molecules: Toward Exact Energetics for Supramolecular Systems. *J. Phys. Chem. Lett.* **2014**, *5*, 849–855.
- (84) Benali, A.; Shulenburger, L.; Romero, N. A.; Kim, J.; von Lilienfeld, O. A. Application of Diffusion Monte Carlo to Materials Dominated by van der Waals Interactions. *J. Chem. Theory Comput.* **2014**, *10*, 3417–3422.
- (85) Ceperley, D.; Chester, G. V.; Kalos, M. H. Monte Carlo simulation of a many-fermion study. *Phys. Rev. B* **1977**, *16*, 3081–3099.
- (86) Hammond, B. L.; Reynolds, P. J.; Lester, W. A. Valence quantum Monte Carlo with ab initio effective core potentials. *J. Chem. Phys.* **1987**, *87*, 1130–1136.
- (87) Kosztin, I.; Faber, B.; Schulten, K. Introduction to the diffusion Monte Carlo methods. *Am. J. Phys.* **1996**, *64*, 633–644.
- (88) Lüchow, A.; Anderson, J. B. Monte Carlo methods in electronic structures for large systems. *Annu. Rev. Phys. Chem.* **2000**, *51*, 501.
- (89) Foulkes, W. M. C.; Mitas, L.; Needs, R. J.; Rajagopal, G. Quantum Monte Carlo simulations of solids. *Rev. Mod. Phys.* **2001**, *73*, 33–83.
- (90) Lester, W. A., Jr.; Mitas, L.; Hammond, B. Quantum Monte Carlo for atoms, molecules and solids. *Chem. Phys. Lett.* **2009**, *478*, 1–10.
- (91) Bajdich, M.; Mitas, L. Electronic Structure Quantum Monte Carlo. *Acta Phys. Slovaca* **2009**, *59*, 81–168.
- (92) Needs, R. J.; Towler, M. D.; Drummond, N. D.; López Ríos, P. Continuum variational and diffusion quantum Monte Carlo calculations. *J. Phys.: Condens. Matter* **2010**, *22*, 023201.
- (93) Kolorenč, J.; Mitas, L. Applications of quantum Monte Carlo methods in condensed systems. *Rep. Prog. Phys.* **2011**, *74*, 026502.
- (94) Lüchow, A. Quantum Monte Carlo methods. *WIREs Comput. Mol. Sci.* **2011**, *1*, 388–402.
- (95) Austin, B. M.; Zubarev, D. Y.; Lester, W. A. Quantum Monte Carlo and Related Approaches. *Chem. Rev.* **2012**, *112*, 263–288.
- (96) Morales, M. A.; Clay, R.; Pierleoni, C.; Ceperley, D. M. First Principles Methods: A Perspective from Quantum Monte Carlo. *Entropy* **2014**, *16*, 287–321.
- (97) Wagner, L. K. Quantum Monte Carlo for Ab Initio calculations of energy-relevant materials. *Int. J. Quantum Chem.* **2014**, *114*, 94–101.
- (98) Brown, E.; Morales, M. A.; Pierleoni, C.; Ceperley, D. A. Quantum Monte Carlo Techniques and Applications for Warm Dense Matter. In *Frontiers and Challenges in Warm Dense Matter*; Graziani, F., Ed.; Springer, 2014; pp 123–149.
- (99) Dubeczký, M. Quantum Monte Carlo for Noncovalent Interactions: A Tutorial Review. *Acta Phys. Slovaca* **2014**, *64*, 501–574.
- (100) Gregory, J. K.; Clary, D. C. Structure of Water Clusters. The Contribution of Many-Body Forces, Monomer Relaxation, and Vibrational Zero-Point Energy. *J. Phys. Chem.* **1996**, *100*, 18014–18022.
- (101) Mella, M.; Colombo, M. C.; Morosi, G. Ground state and excitation dynamics in Ag doped helium clusters. *J. Chem. Phys.* **2002**, *117*, 9695.
- (102) Turnbull, J. D.; Boninsegni, M. Adsorption of para-hydrogen on fullerenes. *Phys. Rev. B: Condens. Matter Mater. Phys.* **2005**, *71*, 205421.
- (103) Turnbull, J. D.; Boninsegni, M. Molecular hydrogen isotopes adsorbed on krypton-preplated graphite. *Phys. Rev. B: Condens. Matter Mater. Phys.* **2007**, *76*, 104524.
- (104) Fujita, T.; Tanaka, S.; Fujiwara, T.; Kusa, M.-A.; Mochizuki, Y.; Shiga, M. Ab initio path integral Monte Carlo simulations for water trimer with electron correlation effects. *Comput. Theor. Chem.* **2012**, *997*, 7–13.
- (105) Karlický, F.; Lepetit, B.; Lemoine, D. Quantum modelling of hydrogen chemisorption on graphene and graphite. *J. Chem. Phys.* **2014**, *140*, 124702.
- (106) Davidson, E. R.; Klimeš, J.; Alfè, D.; Michaelides, A. Cooperative interplay of van der Waals forces and quantum nuclear effects on adsorption: H at graphene and at coronene. *ACS Nano* **2014**, *8*, 9905–9913.
- (107) Mallory, J. D.; Brown, S. E.; Mandelshtam, V. A. Assessing the Performance of the Diffusion Monte Carlo Method As Applied to the

- Water Monomer, Dimer, and Hexamer. *J. Phys. Chem. A* **2015**, *119*, 6504–6515.
- (108) Ceperley, D. M.; Alder, B. J. Ground State of the Electron Gas by a Stochastic Method. *Phys. Rev. Lett.* **1980**, *45*, 566–569.
- (109) Schmidt, K. E.; Ceperley, D. M. Monte Carlo Techniques for Quantum Fluids, Solids and Droplets. In *The Monte Carlo Method in Condensed Matter Physics*; Binder, K., Ed.; Springer-Verlag: Berlin, 1992.
- (110) Bacic, Z.; Bowman, J. M. Advances in molecular vibrations and collision dynamics: molecular clusters. In *Advances in Molecular Vibrations and Collision Dynamics*, 1998, *3*, JAI London; <http://cds.cern.ch/record/1991928>.
- (111) McCoy, A. B. Diffusion Monte Carlo approaches for investigating the structure and vibrational spectra of fluxional systems, *Int. Rev. Int. Rev. Phys. Chem.* **2006**, *25* (1–2), 77–107.
- (112) Chang, S. Y.; Bertsch, G. F. Unitary Fermi gas in a harmonic trap. *Phys. Rev. A: At., Mol., Opt. Phys.* **2007**, *76*, 021603(R).
- (113) Umrigar, C. J.; Nightingale, M. P.; Runge, K. J. A diffusion Monte Carlo algorithm with very small time-step errors. *J. Chem. Phys.* **1993**, *99*, 2865–2890.
- (114) Moskowitz, J. W.; Schmidt, K. E.; Lee, M. A.; Kalos, M. H. A new look at correlation energy in atomic and molecular systems. II. The application of the Green's function Monte Carlo method to LiH. *J. Chem. Phys.* **1982**, *77*, 349–355.
- (115) Ortiz, G.; Ceperley, D. M.; Martin, R. M. New stochastic method for systems with broken time-reversal symmetry: 2D fermions in a magnetic field. *Phys. Rev. Lett.* **1993**, *71*, 2777–2780.
- (116) Reynolds, P. J.; Ceperley, D. M.; Alder, B. J.; Lester, W. A., Jr. Fixed-node quantum Monte Carlo for molecules. *J. Chem. Phys.* **1982**, *77*, 5593–5603.
- (117) Petruzielo, F. R.; Toulouse, J.; Umrigar, C. J. Approaching chemical accuracy with quantum Monte Carlo. *J. Chem. Phys.* **2012**, *136*, 12411610.1063/1.3697846.
- (118) Ceperley, D. M. Fermion nodes. *J. Stat. Phys.* **1991**, *63*, 1237–1267.
- (119) Mitas, L. Structure of Fermion Nodes and Nodal Cells. *Phys. Rev. Lett.* **2006**, *96*, 240402.
- (120) Rasch, K. M.; Mitas, L. M. Impact of electron density on the fixed-node errors in Quantum Monte Carlo of atomic systems. *Chem. Phys. Lett.* **2012**, *528*, 59–62.
- (121) Kulahlioglu, A. H.; Rasch, K. M.; Hu, S.; Mitas, L. M. Density dependence of fixed-node errors in diffusion quantum Monte Carlo: Triplet pair correlations. *Chem. Phys. Lett.* **2014**, *591*, 170–174.
- (122) Rasch, K. M.; Hu, S.; Mitas, L. M. Communication: Fixed-node errors in quantum Monte Carlo: Interplay of electron density and node nonlinearities. *J. Chem. Phys.* **2014**, *140*, 041102.
- (123) López Ríos, P.; Seth, P.; Drummond, N. D.; Needs, R. J. Framework for constructing generic Jastrow correlation factors. *Phys. Rev. E* **2012**, *86*, 036703.
- (124) Casula, M.; Attaccalite, C.; Sorella, S. Correlated geminal wave function for molecules: An efficient resonating valence bond approach. *J. Chem. Phys.* **2004**, *121*, 7110.
- (125) Bajdich, M.; Mitas, L.; Drobny, G.; Wagner, L. K.; Schmidt, K. E. Pfaffian Pairing Wave Functions in Electronic-Structure Quantum Monte Carlo Simulations. *Phys. Rev. Lett.* **2006**, *96*, 130201.
- (126) Kwon, Y.; Ceperley, D. M.; Martin, R. M. Effects of backflow correlation in the three-dimensional electron gas: Quantum Monte Carlo study. *Phys. Rev. B: Condens. Matter Mater. Phys.* **1998**, *58*, 6800–6806.
- (127) López Ríos, P.; Ma, A.; Drummond, N. D.; Towler, M. D.; Needs, R. J. Inhomogeneous backflow transformations in quantum Monte Carlo calculations. *Phys. Rev. E* **2006**, *74*, 066701.
- (128) Umrigar, C. J.; Wilson, K. G.; Wilkins, J. W. Optimized trial wave functions for quantum Monte Carlo calculations. *Phys. Rev. Lett.* **1988**, *60*, 1719–1722.
- (129) Umrigar, C. J.; Toulouse, J.; Filippi, C.; Sorella, S.; Hennig, R. G. Alleviation of the Fermion-Sign Problem by Optimization of Many-Body Wave Functions. *Phys. Rev. Lett.* **2007**, *98*, 110201.
- (130) Toulouse, J.; Umrigar, C. J. Full optimization of Jastrow-Slater wave functions with application to the first-row atoms and homonuclear diatomic molecules. *J. Chem. Phys.* **2008**, *128*, 174101.
- (131) Toulouse, J.; Umrigar, C. J. Optimization of quantum Monte Carlo wave functions by energy minimization. *J. Chem. Phys.* **2007**, *126*, 084102.
- (132) Umrigar, C. J.; Filippi, C. Energy and Variance Optimization of Many-Body Wave Functions. *Phys. Rev. Lett.* **2005**, *94*, 150201.
- (133) Trail, J. R. Heavy-tailed random error in quantum Monte Carlo. *Phys. Rev. E* **2008**, *77*, 016703.
- (134) Bajdich, M.; Mitas, L.; Wagner, L. K.; Schmidt, K. E. Pfaffian pairing and backflow wavefunctions for electronic structure quantum Monte Carlo methods. *Phys. Rev. B: Condens. Matter Mater. Phys.* **2008**, *77*, 115112.
- (135) Kolorenč, J.; Hu, S.; Mitas, L. Wave functions for quantum Monte Carlo calculations in solids: Orbitals from density functional theory with hybrid exchange-correlation functionals. *Phys. Rev. B: Condens. Matter Mater. Phys.* **2010**, *82*, 115108.
- (136) Wagner, L. K.; Mitas, L. A quantum Monte Carlo study of electron correlation in transition metal oxygen molecules. *Chem. Phys. Lett.* **2003**, *370*, 412–417.
- (137) Gurtubay, I. G.; Needs, R. J. Dissociation energy of the water dimer from quantum Monte Carlo calculations. *J. Chem. Phys.* **2007**, *127*, 124306.
- (138) Shirley, E. L.; Mitas, L.; Martin, R. M. Core-valence partitioning and quasiparticle pseudopotentials. *Phys. Rev. B: Condens. Matter Mater. Phys.* **1991**, *44*, 3395–3398.
- (139) Ceperley, D. M.; Mitas, L. Monte Carlo methods in quantum chemistry; *Advances in Chemical Physics*; New York, 1996; Vol. XCIII, pp 1–38.
- (140) Hammond, B. L.; Reynolds, P. J.; Lester, W. A., Jr. Valence quantum Monte Carlo with ab initio effective core potentials. *J. Chem. Phys.* **1987**, *87*, 1130.
- (141) Hurley, M. M.; Christiansen, P. A. Relativistic effective potentials in quantum Monte Carlo calculations. *J. Chem. Phys.* **1987**, *86*, 1069.
- (142) Mitáš, L.; Shirley, E. L.; Ceperley, D. M. Nonlocal pseudopotentials and diffusion Monte Carlo. *J. Chem. Phys.* **1991**, *95*, 3467–3475.
- (143) Ceperley, D. M.; Partridge, H. The He₂ potential at small distances. *J. Chem. Phys.* **1986**, *84*, 820–821.
- (144) ten Haaf, D. F. B.; van Bemmelen, H. J. M.; van Leeuwen, J. M. J.; van Saarloos, W.; Ceperley, D. M. Proof for an upper bound in fixed-node Monte Carlo for lattice fermions. *Phys. Rev. B: Condens. Matter Mater. Phys.* **1995**, *51*, 13039–13045.
- (145) Casula, M. Beyond the locality approximation in the standard diffusion Monte Carlo method. *Phys. Rev. B: Condens. Matter Mater. Phys.* **2006**, *74*, 161102(R).
- (146) Williamson, A. J.; Rajagopal, G.; Needs, R. J.; Fraser, L. M.; Foulkes, W. M. C.; Wang, Y.; Chou, M.-Y. Elimination of Coulomb finite-size effects in quantum many-body simulations. *Phys. Rev. B: Condens. Matter Mater. Phys.* **1997**, *55*, R4851–R4854.
- (147) Kent, P. R. C.; Hood, R. Q.; Williamson, A. J.; Needs, R. J.; Foulkes, W. M. C.; Rajagopal, G. Finite-size errors in quantum many-body simulations of extended systems. *Phys. Rev. B: Condens. Matter Mater. Phys.* **1999**, *59*, 1917–1929.
- (148) Azadi, S.; Foulkes, W. M. C. Systematic study of finite-size effects in quantum Monte Carlo calculations of real metallic systems. *J. Chem. Phys.* **2015**, *143*, 102807.
- (149) Shulenburger, L.; Mattsson, T. R. Quantum Monte Carlo applied to solids. *Phys. Rev. B: Condens. Matter Mater. Phys.* **2013**, *88*, 245117.
- (150) Williamson, A. J.; Hood, R. Q.; Grossman, J. C. Linear-Scaling Quantum Monte Carlo Calculations. *Phys. Rev. Lett.* **2001**, *87*, 246406.
- (151) Reboreda, F. A.; Williamson, A. J. Optimized nonorthogonal localized orbitals for linear scaling quantum Monte Carlo calculations. *Phys. Rev. B: Condens. Matter Mater. Phys.* **2005**, *71*, 121105(R).
- (152) Esler, K. P.; Kim, J.; Ceperley, D.; Purwanto, W.; Walter, E.; Krakauer, H.; Zhang, S.; Kent, P.; Hennig, R.; Umrigar, C.; Bajdich, M.; Kolorenč, J.; Mitas, L.; Srinivasan, A. Quantum Monte Carlo algorithms

- for electronic structure at petascale: the Endstation project. *J. Phys.: Conf. Ser.* **2008**, *125*, 012057.
- (153) Nemec, N. Diffusion Monte Carlo: Exponential scaling of computational cost for large systems. *Phys. Rev. B: Condens. Matter Mater. Phys.* **2010**, *81*, 035119.
- (154) Wagner, L. K.; Abbamonte, P. Effect of electron correlation on the electronic structure and spin-lattice coupling of high- T_c cuprates: Quantum Monte Carlo calculations. *Phys. Rev. B: Condens. Matter Mater. Phys.* **2014**, *90*, 125129.
- (155) Wagner, L. K. Ground state of doped cuprates from first-principles quantum Monte Carlo calculations. *Phys. Rev. B: Condens. Matter Mater. Phys.* **2015**, *92*, 161116.
- (156) Foyevtsova, K.; Krogel, J. T.; Kim, J.; Kent, P. R. C.; Dagotto, E.; Reboreda, F. A. *Ab initio* Quantum Monte Carlo Calculations of Spin Superexchange in Cuprates: The Benchmarking Case of Ca_2CuO_3 . *Phys. Rev. X* **2014**, *4*, 031003.
- (157) Zheng, H.; Wagner, L. K. Computation of the Correlated Metal-Insulator Transition in Vanadium Dioxide from First Principles. *Phys. Rev. Lett.* **2015**, *114*, 176401.
- (158) Tkatchenko, A.; Alfe, D.; Kim, K. S. First-Principles Modeling of Non-Covalent Interactions in Supramolecular Systems: The Role of Many-Body Effects. *J. Chem. Theory Comput.* **2012**, *8*, 4317–4322.
- (159) Mostaani, E.; Drummond, N. D.; Fal'ko, V. I. Quantum Monte Carlo Calculation of the Binding Energy of Bilayer Graphene. *Phys. Rev. Lett.* **2015**, *115*, 115501.
- (160) Al-Hamdan, Y. S.; Ma, M.; Alfe, D.; von Lilienfeld, O. A.; Michaelides, A. Communication: Water on hexagonal boron nitride from diffusion Monte Carlo. *J. Chem. Phys.* **2015**, *142*, 181101.
- (161) Wu, Y.; Wagner, L. K.; Narayana, R. A. The interaction between hexagonal boron nitride and water from first principles. *J. Chem. Phys.* **2015**, *142*, 234702.
- (162) Zhang, S.; Krakauer, H. Quantum Monte Carlo Method using Phase-Free Random Walks with Slater Determinants. *Phys. Rev. Lett.* **2003**, *90*, 136401.
- (163) Booth, G. H.; Thom, A. J. W.; Alavi, A. Fermion Monte Carlo without fixed nodes: a game of Life, death and annihilation in Slater determinant space. *J. Chem. Phys.* **2009**, *131*, 054106.
- (164) Neuscammman, E. Communication: A Jastrow factor coupled cluster theory for weak and strong electron correlation. *J. Chem. Phys.* **2013**, *139*, 181101.
- (165) Neuscammman, E. The Jastrow antisymmetric geminal power in Hilbert space: Theory, benchmarking, and application to a novel transition state. *J. Chem. Phys.* **2013**, *139*, 194105.
- (166) Wouters, S.; Verstichel, B.; Van Neck, D.; Chan, G. K.-L. Projector quantum Monte Carlo with matrix product states. *Phys. Rev. B: Condens. Matter Mater. Phys.* **2014**, *90*, 045104.
- (167) Booth, G. H.; Grüneis, A.; Kresse, G.; Alavi, A. Towards an exact description of electronic wavefunctions in real solids. *Nature* **2012**, *493*, 365–370.
- (168) Purwanto, W.; Al-Saidi, W. A.; Krakauer, H.; Zhang, S. Eliminating spin contamination in auxiliary-field quantum Monte Carlo: Realistic potential energy curve of F_2 . *J. Chem. Phys.* **2008**, *128*, 114309.
- (169) Ma, F.; Zhang, S.; Krakauer, H. Excited state calculations in solids by auxiliary-field quantum Monte Carlo. *New J. Phys.* **2013**, *15*, 093017.
- (170) Scemama, A.; Appelcourt, T.; Giner, E.; Caffarel, M. Accurate nonrelativistic ground-state energies of 3d transition metal atoms. *J. Chem. Phys.* **2014**, *141*, 244110.
- (171) Caffarel, M.; Giner, E.; Scemama, A.; Ramírez-Solís, A. Spin Density Distribution in Open-Shell Transition Metal Systems: A Comparative Post-Hartree-Fock, Density Functional Theory, and Quantum Monte Carlo Study of the CuCl_2 Molecule. *J. Chem. Theory Comput.* **2014**, *10*, 5286–5296.
- (172) Giner, E.; Scemama, A.; Caffarel, M. Fixed-Node Diffusion Monte Carlo potential energy curve of the fluorine molecule F_2 using selected configuration interaction trial wavefunctions. *J. Chem. Phys.* **2015**, *142*, 044115.
- (173) QMCPACK. <http://qmcpack.org/> (accessed April 1, 2016).
- (174) Wagner, L. K.; Bajdich, M.; Mitas, L. QWalk: A quantum Monte Carlo program for electronic structure. *J. Comput. Phys.* **2009**, *228*, 3390–3404. <http://www.qwalk.org/>.
- (175) Needs, R. J.; Towler, M. D.; Drummond, N. D.; López Ríos, P. *CASINO User's Guide Version 2.13*; University of Cambridge: Cambridge, UK, 2015, <http://www.tcm.phy.cam.ac.uk/~mdt26/casino2.html>.
- (176) CHAMP. <http://pages.physics.cornell.edu/~cyrus/champ.html> (accessed April 1, 2016).
- (177) Santra, B.; Michaelides, A.; Fuchs, M.; Tkatchenko, A.; Filippi, C.; Scheffler, M. On the accuracy of density-functional theory exchange-correlation functionals for H bonds in small water clusters. II. The water hexamer and van der Waals interactions. *J. Chem. Phys.* **2008**, *129*, 194111.
- (178) Ma, J.; Alfe, D.; Michaelides, A.; Wang, E. The water-benzene interaction: Insight from electronic structure theories. *J. Chem. Phys.* **2009**, *130*, 154303.
- (179) Korth, M.; Grimme, S.; Towler, M. D. The Lithium-Thiophene Riddle Revisited. *J. Phys. Chem. A* **2011**, *115*, 11734–11739.
- (180) Manten, S.; Lüchow, A. On the accuracy of the fixed-node diffusion quantum Monte Carlo method. *J. Chem. Phys.* **2001**, *115*, 5362–5366.
- (181) Grossman, J. C. Benchmark quantum Monte Carlo calculations. *J. Chem. Phys.* **2002**, *117*, 1434–1440.
- (182) Nemec, N.; Towler, M. D.; Needs, R. J. Benchmark all-electron ab initio quantum Monte Carlo calculations for small molecules. *J. Chem. Phys.* **2010**, *132*, 034111.
- (183) Morales, M. A.; McMinis, J.; Clark, B. K.; Kim, J.; Scuseria, G. E. Multideterminant Wave Functions in Quantum Monte Carlo. *J. Chem. Theory Comput.* **2012**, *8*, 2181–2188.
- (184) Benedek, N. A.; Snook, I. K.; Towler, M. D.; Needs, R. J. Quantum Monte Carlo calculations of the dissociation energy of the water dimer. *J. Chem. Phys.* **2006**, *125*, 104302.
- (185) Drummond, N. D.; Monserrat, B.; Lloyd-Williams, J. H.; López Ríos, P.; Pickard, C. J.; Needs, R. J. Quantum Monte Carlo study of the phase diagram of solid molecular hydrogen at extreme pressures. *Nat. Commun.* **2014**, *6*, 7794.
- (186) Clay, R.; Morales, M. A. Influence of single particle orbital sets and configuration selection on multideterminant wavefunctions in quantum Monte Carlo. *J. Chem. Phys.* **2015**, *142*, 234103.
- (187) Lawson, J. W.; Bauschlicher, C. W., Jr.; Toulouse, J.; Filippi, C.; Umrigar, C. J. Quantum Monte Carlo study of the cooperative binding of NO_2 to fragment models of carbon nanotubes. *Chem. Phys. Lett.* **2008**, *466*, 170–175.
- (188) Bajdich, M.; Reboreda, F. A.; Kent, P. R. C. Quantum Monte Carlo calculations of dihydrogen binding energetics on Ca cations: An assessment of errors in density functionals for weakly bonded systems. *Phys. Rev. B: Condens. Matter Mater. Phys.* **2010**, *82*, 081405(R).
- (189) Harkless, J. A. W.; Irikura, K. K. Multi-determinant Trial Functions in the Determination of the Dissociation Energy of the Beryllium Dimer: Quantum Monte Carlo Study. *Int. J. Quantum Chem.* **2006**, *106*, 2373–2378.
- (190) Deible, M. J.; Kessler, M.; Gasperich, K. E.; Jordan, K. D. Quantum Monte Carlo calculation of the binding energy of the beryllium dimer. *J. Chem. Phys.* **2015**, *143*, 084116.
- (191) Hongo, K.; Cuong, N. T.; Maezono, R. The Importance of Electron Correlation on Stacking Interaction of Adenine-Thymine Base-Pair Step in BDNA: A Quantum Monte Carlo Study. *J. Chem. Theory Comput.* **2013**, *9*, 1081–1086.
- (192) Shulenburger, L.; Desjarlais, M. P.; Mattsson, T. R. Theory of melting at high pressures: Amending density functional theory with quantum Monte Carlo. *Phys. Rev. B: Condens. Matter Mater. Phys.* **2014**, *90*, 140104(R).
- (193) Hongo, K.; Watson, M. A.; S, R.; Itaka, T.; Aspuru-Guzik, A.; Maezono, R. Diffusion Monte Carlo Study of Para-Diiodobenzene Polymorphism Revisited. *J. Chem. Theory Comput.* **2015**, *11*, 907–917.
- (194) Springall, R.; Per, M. C.; Russo, S. P.; Snook, I. K. Quantum Monte Carlo calculations of the potential energy curve of the helium dimer. *J. Chem. Phys.* **2008**, *128*, 114308.

- (195) Wu, X.; Hu, X.; Dai, Y.; Du, C.; Chu, S.; Hu, L.; Deng, J.; Feng, Y. Quantum Monte Carlo calculated potential energy curve for the helium dimer. *J. Chem. Phys.* **2010**, *132*, 204304.
- (196) Grimme, S.; Diedrich, C.; Korth, M. The Importance of Inter- and Intramolecular van der Waals Interactions in Organic Reactions: the Dimerization of Anthracene Revisited. *Angew. Chem., Int. Ed.* **2006**, *45*, 625–629.
- (197) Kim, Y.-H.; Zhao, Y.; Williamson, A.; Heben, M. J.; Zhang, S. B. Nondissociative Adsorption of H₂ Molecules in Light-Element-Doped Fullerenes. *Phys. Rev. Lett.* **2006**, *96*, 016102.
- (198) Gurtubay, I. G.; Drummond, N. D.; Towler, M. D.; Needs, R. J. Quantum Monte Carlo calculations of the dissociation energies of three-electron hemibonded radical cationic dimers. *J. Chem. Phys.* **2006**, *124*, 024318.
- (199) Zucchetti, M.; Filippi, C.; Buda, F. Anion- π and π - π Cooperative Interactions Regulating the Self-Assembly of Nitrate-Triazine-Triazine Complexes. *J. Phys. Chem. A* **2008**, *112*, 1627–1632.
- (200) Wu, Z.; Allendorf, M. D.; Grossman, J. C. Quantum Monte Carlo Simulation of Nanoscale MgH₂ Cluster Thermodynamics. *J. Am. Chem. Soc.* **2009**, *131*, 13918–13919.
- (201) Cox, S. J.; Towler, M. D.; Alfè, D.; Michaelides, A. Benchmarking the performance of density functional theory and point charge force fields in their description of sI methane hydrate against diffusion Monte Carlo. *J. Chem. Phys.* **2014**, *140*, 174703.
- (202) Deible, M. J.; Tuguldur, O.; Jordan, K. D. Theoretical Study of the Binding Energy of a Methane Molecule in a (H₂O)₂₀ Dodecahedral Cage. *J. Phys. Chem. B* **2014**, *118*, 8257–8263.
- (203) Per, M. C.; Walker, K. A.; Russo, S. P. How Important is Orbital Choice in Single-Determinant Diffusion Quantum Monte Carlo Calculations? *J. Chem. Theory Comput.* **2012**, *8*, 2255–2259.
- (204) Beaudet, T. D.; Casula, M.; Kim, J.; Sorella, S.; Martin, R. M. Molecular hydrogen adsorbed on benzene: Insights from a quantum Monte Carlo study. *J. Chem. Phys.* **2008**, *129*, 164711.
- (205) Bianchi, R.; Bressanini, D.; Cremaschi, P.; Mella, M.; Morosi, G. Wave-Function Optimization by Least-Squares Fitting of the Exact Wave Function Sampled by Quantum Monte Carlo. *Int. J. Quantum Chem.* **1996**, *57*, 321–325.
- (206) Xu, J.; Deible, M. J.; Peterson, K. A.; Jordan, K. D. Correlation Consistent Gaussian Basis Sets for H, B–Ne with Dirac-Fock AREP Pseudopotentials: Applications in Quantum Monte Carlo Calculations. *J. Chem. Theory Comput.* **2013**, *9*, 2170–2178.
- (207) Hachmann, J.; Galek, P. T. A.; Yanai, T.; Chan, G. K.-L.; Handy, N. C. The nodes of Hartree-Fock wavefunctions and their orbitals. *Chem. Phys. Lett.* **2004**, *392*, 55–61.
- (208) Bande, A.; Lüchow, A.; Della Sala, F.; Görling, A. Rydberg states with quantum Monte Carlo. *J. Chem. Phys.* **2006**, *124*, 114114.
- (209) Dunning, T. H., Jr. Gaussian basis sets for use in correlated molecular calculations. I. The atoms boron through neon and hydrogen. *J. Chem. Phys.* **1989**, *90*, 1007–1023.
- (210) Wang, F.-F.; Deible, M. J.; Jordan, K. D. Benchmark Study of the Interaction Energy for an (H₂O)₁₆ Cluster: Quantum Monte Carlo and Complete Basis Set Limit MP2 Results. *J. Phys. Chem. A* **2013**, *117*, 7606–7611.
- (211) Ma, J.; Michaelides, A.; Alfè, D. Binding of hydrogen on benzene, coronene, and graphene from quantum Monte Carlo calculations. *J. Chem. Phys.* **2011**, *134*, 134701.
- (212) Karalti, O.; Alfè, D.; Gillan, M. J.; Jordan, K. D. Adsorption of a water molecule on the MgO(100) surface as described by cluster and slab models. *Phys. Chem. Chem. Phys.* **2012**, *14*, 7846–7853.
- (213) Ambrosetti, A.; Silvestrelli, P.; Toigo, F.; Mitas, L.; Pederiva, F. Variational Monte Carlo for spin-orbit interacting systems. *Phys. Rev. B: Condens. Matter Mater. Phys.* **2012**, *85*, 045115.
- (214) Ganesh, P.; Kim, J.; Park, C.; Yoon, M.; Reboreda, F. A.; Kent, P. R. C. Binding and Diffusion of Lithium in Graphite: Quantum Monte Carlo Benchmarks and Validation of van der Waals Density Functional Methods. *J. Chem. Theory Comput.* **2014**, *10*, 5318–5323.
- (215) Chen, J.; Ren, X.; Li, X.-Z.; Alfè, D.; Wang, E. On the room-temperature phase diagram of high pressure hydrogen: An ab initio molecular dynamics perspective and a diffusion Monte Carlo study. *J. Chem. Phys.* **2014**, *141*, 024501.
- (216) Snajdr, M.; Rothstein, S. M. Are properties derived from variance-optimized wave functions generally more accurate? Monte Carlo study of non-energy-related properties of H₂, He, and LiH. *J. Chem. Phys.* **2000**, *112*, 4935–4941.
- (217) Hsing, C. R.; Wei, C. M.; Chou, M. Y. Quantum Monte Carlo investigations of adsorption energetics on graphene. *J. Phys.: Condens. Matter* **2012**, *24*, 395002.
- (218) Jiang, X.; Cheng, X.; Chen, G.; Zhang, H. Diffusion Monte Carlo Study of the Hydrogen Molecules Adsorbed on C₄H₃Li. *Int. J. Quantum Chem.* **2012**, *112*, 2627–2631.
- (219) Drummond, N. D.; Needs, R. J. Quantum Monte Carlo, density functional theory, and pair potential studies of solid neon. *Phys. Rev. B: Condens. Matter Mater. Phys.* **2006**, *73*, 024107.
- (220) Santra, B.; Klimeš, J.; Alfè, D.; Tkatchenko, A.; Slater, B.; Michaelides, A.; Car, R.; Scheffler, M. Hydrogen Bonds and van der Waals Forces in Ice at Ambient and High Pressures. *Phys. Rev. Lett.* **2011**, *107*, 185701.
- (221) Raza, Z.; Alfè, D.; Salzmann, C. G.; Klimeš, J.; Michaelides, A.; Slater, B. Proton ordering in cubic ice and hexagonal ice: a potential new ice phase - XIc. *Phys. Chem. Chem. Phys.* **2011**, *13*, 19788–19795.
- (222) Gillan, M. J.; Alfè, D.; Bartók, A. P.; Csányi, G. First-principles energetics of water clusters and ice: A many-body analysis. *J. Chem. Phys.* **2013**, *139*, 244504.
- (223) Xu, J.; Jordan, K. D. Application of the Diffusion Monte Carlo Method to the Binding of Excess Electrons to Water Clusters. *J. Phys. Chem. A* **2010**, *114*, 1364–1366.
- (224) Natoli, V.; Martin, R. M.; Ceperley, D. Crystal Structure of Molecular Hydrogen at High Pressure. *Phys. Rev. Lett.* **1995**, *74*, 1601–1604.
- (225) Attaccalite, C.; Sorella, S. Stable Liquid Hydrogen at High Pressure by a Novel Ab Initio Molecular-Dynamics Calculation. *Phys. Rev. Lett.* **2008**, *100*, 114501.
- (226) Morales, M. A.; Pierleoni, C.; Schwegler, E.; Ceperley, D. M. Evidence for a first-order liquid-liquid transition in high-pressure hydrogen from ab initio simulations. *Proc. Natl. Acad. Sci. U. S. A.* **2010**, *107*, 12799–12803.
- (227) Mazzola, G.; Yunoki, S.; Sorella, S. Unexpectedly high pressure for molecular dissociation in liquid hydrogen by electronic simulation. *Nat. Commun.* **2014**, *5*, 3487.
- (228) McMinis, J.; Clay, R. C., III; Lee, D.; Morales, M. A. Molecular to Atomic Phase Transition in Hydrogen under High Pressure. *Phys. Rev. Lett.* **2015**, *114*, 105305.
- (229) Tubman, N. M.; Liberatore, E.; Pierleoni, C.; Holzmann, M.; Ceperley, D. M. Molecular-Atomic Transition along the Deuterium Hugoniot Curve with Coupled Electron-Ion Monte Carlo Simulations. *Phys. Rev. Lett.* **2015**, *115*, 045301.
- (230) Pang, T. Properties of ionic hydrogen clusters: a quantum Monte Carlo study. *Chem. Phys. Lett.* **1994**, *228*, 555–561.
- (231) Bokes, P.; Stich, I.; Mitas, L. Electron Correlation Effects in Ionic Hydrogen Clusters. *Int. J. Quantum Chem.* **2001**, *83*, 86–95.
- (232) Kocman, M.; Jurečka, P.; Dubecký, M.; Otyepka, M.; Cho, Y.; Kim, K. S. Choosing a density functional for modeling adsorptive hydrogen storage: reference quantum mechanical calculations and a comparison of dispersion-corrected density functionals. *Phys. Chem. Chem. Phys.* **2015**, *17*, 6423–6432.
- (233) Bhattacharya, A.; Anderson, J. Exact quantum Monte Carlo calculation of the H-He interaction potential. *Phys. Rev. A: At., Mol., Opt. Phys.* **1994**, *49*, 2441–2442.
- (234) Clay, R. C., III; Holzmann, M.; Ceperley, D. M.; Morales, M. A. Benchmarking density functionals for hydrogen-helium mixtures with quantum Monte Carlo: Energetics, pressures, and forces. *Phys. Rev. B: Condens. Matter Mater. Phys.* **2016**, *93*, 035121.
- (235) Mohan, V.; Anderson, J. Quantum Monte Carlo calculations of three-body corrections in the interaction of three helium atoms. *J. Chem. Phys.* **1990**, *92*, 6971–6973.

- (236) Anderson, J. B.; Traynor, C. A.; Boghosian, B. M. An exact quantum Monte Carlo calculation of helium-helium intermolecular potential. *J. Chem. Phys.* **1993**, *99*, 345–351.
- (237) Bhattacharya, A.; Anderson, J. B. The interaction potential of a symmetric helium trimer. *J. Chem. Phys.* **1994**, *100*, 8999–9001.
- (238) Anderson, J. B. An exact quantum Monte Carlo calculation of the helium-helium intermolecular potential. II. *J. Chem. Phys.* **2001**, *115*, 4546–4548.
- (239) Anderson, J. B. Comment on "An exact quantum Monte Carlo calculation of the helium-helium intermolecular potential" [J. Chem. Phys. **115**, 4546 (2001)]. *J. Chem. Phys.* **2004**, *120*, 9886–9887.
- (240) Huiszoon, C.; Caffarel, M. A quantum Monte Carlo perturbational study of the He-He interaction. *J. Chem. Phys.* **1996**, *104*, 4621–4631.
- (241) Sterpone, F.; Spanu, L.; Ferraro, L.; Sorella, S.; Guidoni, L. Dissecting the Hydrogen Bond: A Quantum Monte Carlo Approach. *J. Chem. Theory Comput.* **2008**, *4*, 1428–1434.
- (242) Alfè, D.; Bartók, A. P.; Csányi, G.; Gillan, M. J. Communication: Energy benchmarking with quantum Monte Carlo for water nanodroplets and bulk liquid water. *J. Chem. Phys.* **2013**, *138*, 221102.
- (243) Alfè, D.; Bartók, A. P.; Csányi, G.; Gillan, M. J. Analyzing the errors of DFT approximations for compressed water systems. *J. Chem. Phys.* **2014**, *141*, 014104.
- (244) Morales, M. A.; Gergely, J. R.; McMinis, J.; McMahon, J. M.; Kim, J.; Ceperley, D. M. Quantum Monte Carlo Benchmark of Exchange-Correlation Functionals for Bulk Water. *J. Chem. Theory Comput.* **2014**, *10*, 2355–2362.
- (245) Quigley, D.; Alfè, D.; Slater, B. Communication: On the stability of ice 0, ice i, and I_v. *J. Chem. Phys.* **2014**, *141*, 161102.
- (246) Grossman, J. C.; Mitas, L. M. Efficient Quantum Monte Carlo Energies for Molecular Dynamics Simulations. *Phys. Rev. Lett.* **2005**, *94*, No. 056403.
- (247) Ma, J.; Michaelides, A.; Alfè, D.; Schimka, L.; Kresse, G.; Wang, E. Adsorption and diffusion of water on graphene from first principles. *Phys. Rev. B: Condens. Matter Mater. Phys.* **2011**, *84*, No. 033402.
- (248) Sorella, S.; Casula, M.; Rocca, D. Weak binding between two aromatic rings: Feeling the van der Waals attraction by quantum Monte Carlo methods. *J. Chem. Phys.* **2007**, *127*, 014105.
- (249) Azadi, S.; Cohen, R. E. Chemical Accuracy from quantum Monte Carlo for the benzene dimer. *J. Chem. Phys.* **2015**, *143*, 104301.
- (250) Kanai, Y.; Grossman, J. C. Role of exchange in density-functional theory for weakly interacting systems: Quantum Monte Carlo analysis of electron density and interaction energy. *Phys. Rev. A: At., Mol., Opt. Phys.* **2009**, *80*, No. 032504.
- (251) Spanu, L.; Sorella, S.; Galli, G. Nature and Strength of Interlayer Binding in Graphite. *Phys. Rev. Lett.* **2009**, *103*, No. 196401.
- (252) Cicero, G.; Grossman, J. C.; Galli, G. Adhesion of single functional groups to individual carbon nanotubes: Electronic effects probed by ab initio calculations. *Phys. Rev. B: Condens. Matter Mater. Phys.* **2006**, *74*, No. 035425.
- (253) Amovilli, C.; Floris, F. M.; Grisafi, A. Localized Polycentric Orbital Basis Set for Quantum Monte Carlo Calculations Derived from the Decomposition of Kohn-Sham Optimized Orbitals. *Computation* **2016**, *4*, 10.
- (254) Caffarel, M.; Scemama, A.; Ramírez-Solís, A. The lithium-thiophene interaction: a critical study using highly correlated electronic structure approaches of quantum chemistry. *Theor. Chem. Acc.* **2010**, *126*, 275–287.
- (255) Horváthová, L.; Dubecký, M.; Mitas, L.; Štich, L. Spin Multiplicity and Symmetry Breaking in Vanadium-Benzene Complexes. *Phys. Rev. Lett.* **2012**, *109*, No. 053001.
- (256) Horváthová, L.; Dubecký, M.; Mitas, L.; Štich, L. Quantum Monte Carlo Study of π -Bonded Transition Metal Organometallics: Neutral and Cationic Vanadium-Benzene and Cobalt-Benzene Half Sandwiches. *J. Chem. Theory Comput.* **2013**, *9*, 390–400.
- (257) Granatier, J.; Dubecký, M.; Lazar, P.; Otyepka, M.; Hobza, P. Spin-Crossing in an Organometallic Pt-Benzene Complex. *J. Chem. Theory Comput.* **2013**, *9*, 1461–1468.
- (258) Hsing, C.-R.; Cheng, C.; Chou, J.-P.; Chang, C.-M.; Wei, C.-M. Van der Waals interaction in a boron nitride bilayer. *New J. Phys.* **2014**, *16*, 113015.
- (259) Drummond, N. D.; Needs, R. J. van der Waals Interactions between Thin Metallic Wires and Layers. *Phys. Rev. Lett.* **2007**, *99*, 166401.
- (260) Filippi, C.; Healy, S. B.; Kratzer, P.; Pehlke, E.; Scheffler, M. Quantum Monte Carlo Calculations of H₂ Dissociation on Si(001). *Phys. Rev. Lett.* **2002**, *89*, 166102.
- (261) Hongo, K.; Watson, M. A.; Sánchez-Carrera, R. S.; Iitaka, T.; Aspuru-Guzik, A. Failure of Conventional Density Functionals for the Prediction of Molecular Crystal Polymorphism: A Quantum Monte Carlo Study. *J. Phys. Chem. Lett.* **2010**, *1*, 1789–1794.
- (262) El Khatib, M.; Bendazzoli, G. L.; Evangelisti, S.; Helal, W.; Leininger, T.; Tenti, L.; Angeli, C. Beryllium Dimer: A Bond Based on Non-Dynamical Correlation. *J. Phys. Chem. A* **2014**, *118*, 6664–6673.
- (263) Lesiuk, M.; Przybytek, M.; Musial, M.; Jeziorski, B.; Moszynski, R. Reexamination of the calculation of two-center, two-electron integrals over Slater-type orbitals. III. Case study of the beryllium dimer. *Phys. Rev. A: At., Mol., Opt. Phys.* **2015**, *91*, No. 012510.
- (264) Anderson, A. G.; Goddard, W. A. III Generalized valence bond wave functions in Quantum Monte Carlo. *J. Chem. Phys.* **2010**, *132*, 164110.
- (265) Caffarel, M.; Hess, O. Quantum Monte Carlo perturbation calculations of interaction energies. *Phys. Rev. A* **1991**, *43*, 2139–2151.
- (266) Misquitta, A. J.; Maezono, R.; Drummond, N. D.; Stone, A. J.; Needs, R. J. Anomalous nonadditive dispersion interactions in systems of three one-dimensional wires. *Phys. Rev. B: Condens. Matter Mater. Phys.* **2014**, *89*, 045140.
- (267) Zen, A.; Luo, Y.; Mazzola, G.; Guidoni, L.; Sorella, S. Ab initio molecular dynamics simulation of liquid water by quantum Monte Carlo. *J. Chem. Phys.* **2015**, *142*, 144111.
- (268) Mazziotti, D. A. Parametrization of the two-electron reduced density matrix for its direct calculation without the many-electron wave function. *Phys. Rev. Lett.* **2008**, *101*, No. 253002.
- (269) DePrince, A. E.; Kamarchik, E.; Mazziotti, D. A. Parametric two-electron reduced-density-matrix method applied to computing molecular energies and properties at nonequilibrium geometries. *J. Chem. Phys.* **2008**, *128*, 234103.
- (270) Mazziotti, D. A. Two-Electron Reduced Density Matrix as the Basic Variable in Many-Electron Quantum Chemistry and Physics. *Chem. Rev.* **2012**, *112*, 244–262.
- (271) Chan, G. K.-L.; Head-Gordon, M. Highly correlated calculations with a polynomial cost algorithm: A study of the density matrix renormalization group. *J. Chem. Phys.* **2002**, *116*, 4462.
- (272) Chan, G. K.-L. An algorithm for large scale density matrix renormalization group calculations. *J. Chem. Phys.* **2004**, *120*, 3172.
- (273) Sharma, S.; Chan, G. K.-L. Spin-adapted density matrix renormalization group algorithms for quantum chemistry. *J. Chem. Phys.* **2012**, *136*, 124121.